UNIVERSIDAD D SEVILLA

Facultad de Matemáticas

Departamento de Ecuaciones Diferenciales y Análisis Numérico

Trabajo de Fin de Grado

Analysis and simulation of some ODE and PDE models used in neuroscience

Autor:

Alejandro Barea Moreno

Dirigido por:

José Antonio Langa Rosado
Antonio Suárez Fernández

Curso 2022/2023

A mamá, a papá y a mi siempre presente amigo Javi.

Brain, *n.* An apparatus with which we think that we think.

Ambrose Bierce, *The Devil's Dictionary*

Index

Resumen

El objetivo de este trabajo es introducir al lector en algunos modelos de EDOs y EDPs que permiten estudiar el comportamiento de la dinámica en el cerebro. Se partirá de algunas hipótesis físicas del comportamiento de las neuronas para deducir modelos que pasarán a ser estudiados cualitativamente y resueltos numéricamente. Posteriormente, se utilizarán aproximaciones para reducir la dimensionalidad y mejorar el análisis para, finalmente, conseguir entender el comportamiento de redes neuronales bajo estímulos estocásticos mediante el uso de la ecuación de Fokker-Planck y de la teoría de ecuaciones diferenciales estocásticas.

Abstract

The aim of this work is to introduce the reader to some models of ODEs and PDEs that allow us to study the behaviour of the dynamics in the brain. We will start from some physical hypotheses of the behaviour of neurons to deduce models that will be studied qualitatively and solved numerically. Subsequently, approximations will be used to reduce dimensionality and improve the analysis in order to finally understand the behaviour of neuronal networks under stochastic stimuli through the use of the Fokker-Planck equation and the theory of stochastic differential equations.

Part 1. The neuron: ion diffusion and action potentials

We will dedicate this first part to understand the voltage of neurons. In Chapter 1, we will consider the physical properties of the cellular medium in order to obtain a set of equations, which will then be used to produce simulations. We will simplify these equations in Chapter 2 to a 2D system which is analytically tractable. Finally, in Chapter 3, the 2D system will be further simplified to obtain the Integrate-and-Fire models, single equations which will prove to be very useful in the second part of this work in the end.

To understand the work it is necessary to have previous knowledge of the theory of differential equations and their qualitative analysis. The theorems and definitions that will be used throughout the work and that are assumed to have been studied along the degree in Mathematics will be included in an appendix at the end.

Chapter 1: The Hodgkin-Huxley equations

Alan Hodgkin and Andrew Huxley, two British researchers at Cambridge University, were awarded the Nobel Prize of Medicine in 1963 due to their articles published in 1952 regarding the propagation of action potentials in a squid's axon. They developed a mathematical framework to understand the change in the potential between the interior and the exterior of cells that have since opened the field of **Computational neuroscience**. In this first Chapter, we will follow the reasoning they used to write their articles.

1.1. Anatomy of a neuron

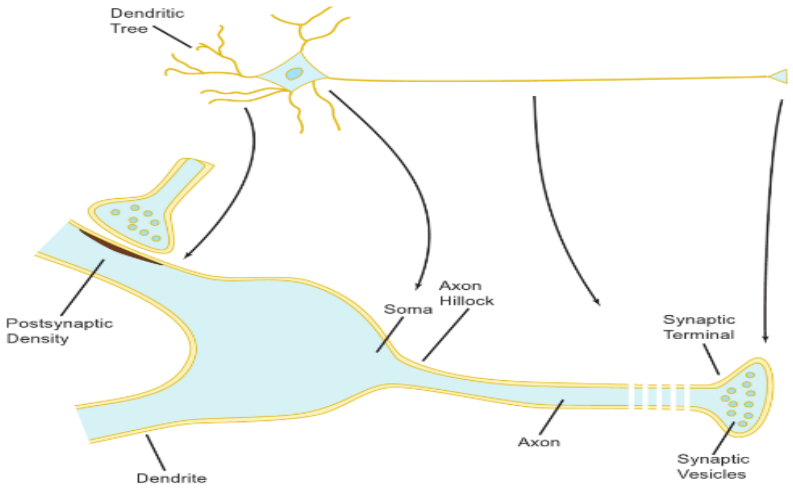

Fig. 1: Parts of a neuron [1].

First, it is necessary to know some of the biology underlying the processes that will be analyzed.

Starting from the basics, a neuron is the basic cell of the nervous system, responsible for the **homeostasis**, which is the equilibrium and coordination of the different parts of the body.

As the figure 1 shows, the neuron is not a homogeneous cell as it has very differentiated parts. Neurons communicate using **action potentials** which are waves of voltage that travel across the membrane to the synaptic terminals. When they arrive there, the synaptic vesicles release neurotransmitters, chemicals that arrive at other neurons' dendritic tree and generate **post-synaptic potentials** which are new action potentials in the activated cells.

1.2. Ion Diffusion and Nernst potential

In the cellular medium, there are a lot of ions of different chemical species: Na^+, K^+, Cl^-, etc... We can quantify the difference in voltage generated by the imbalance in the number of ions inside and outside the cell:

$$V_M = V_{in} - V_{out}$$

when this voltage surpasses a threshold, an action potential is started. The underlying mechanism of this phenomenon will be thoroughly explained throughout this chapter.

Ions move across the cell's membrane through the so-called **ion channels** which are proteins that allow the passing of some selective ions. There are hundreds of channels, but we will focus on the sodium and potassium ones, as they are the most important to determine the cell's voltage.

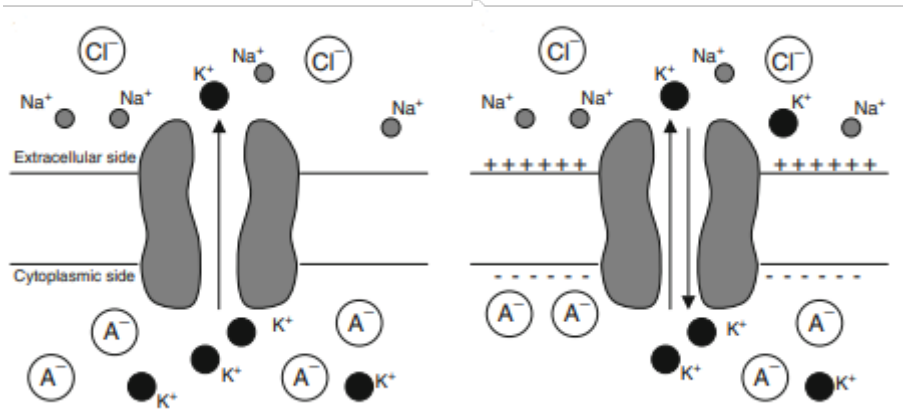

Fig. 2: Ion movement through a cell's membrane [2].

These ions are subjected to two different forces which will determine their movement through the membrane: diffusion and electric drift.

The density of current due to the action of the electric field on the ions (drift) is easily obtained using Ohm's Law:

$$\vec{j}_{drift} = q_t \, \vec{E} = -c \, \mu_q \, \nabla V \tag{1}$$

where q_t is the total charge of the ions travelling through the channel (C), c is the concentration ($kg \cdot m^{-3}$), μ_q the electrical mobility ($m^2 \cdot V^{-1} \cdot s^{-1}$).

Diffusion is a phenomenon originating from the Brownian (random) motion of the particles in the liquid. When observing a gradient of concentration in a chemical species, the spontaneous motion of the particles macroscopically is towards the zone of less concentration. The action of special enzymes called bombs will maintain this concentration gradient, but this will not interfere with our analysis.

Mathematically this is modelled by the first of Fick's Laws:

$$\vec{j}_{diff} = -D\,\nabla c \tag{2}$$

where c is the concentration and D is the diffusion constant ($m^2 \cdot s^{-1}$). Einstein found that this constant is related to the mobility of the ions (μ_q):

$$D = \frac{\mu_q\, k_B\, T}{q} = \frac{\mu_q\, k_B\, T}{ze} \tag{3}$$

where $k_B = 1.38 \cdot 10^{-23}\, m^2 \cdot kg \cdot s^{-2} \cdot K^{-1}$ is the Boltzmann's constant, T the temperature (K) and $e = 1.6 \cdot 10^{-19}\, C$ the elementary charge, which is the net charge of a proton or an electron. The z in this equation is the valence of the ions, which is the number of net charges that it contains, as the ion can have an excess or a defect of electrons, z is an entire number.

Now, if we assume there is no interaction between ions in a channel and that this channel is approximately unidimensional, we can sum (1) and (2) and use (3) to obtain:

$$j_T = -\mu_q c \frac{dV}{dx} - \frac{\mu_q k_B T}{ze} \frac{dc}{dx}. \tag{4}$$

Which is the total density of flux of ions through the channel.

As we have assumed that the channel is unidimensional, the gradients are reduced to derivatives in the spatial variable x which represents the length of the channel.

It will be interesting to know the value of the voltage needed to stop the flow of a particular ion, which will be easily obtained by equating (4) to zero and then integrating between the inside and outside of the cell:

$$E_i = \frac{k_B T}{z_i e} \ln\left(\frac{c_{in,i}}{c_{out,i}}\right).$$

This is the **Nernst Potential** of the ion i.

This potential represents the membrane voltage at which the flux of that particular ion is stopped, which will be illustrated in the next section.

1.3. The equivalent circuit

We are ready now for the first of the equations that will be presented in this work. This one will be useful to understand the behaviour of the membrane potential in the so-called sub-threshold regime, this is the behaviour of the membrane voltage when an action potential hasn't fired yet.

The cell's membrane has the ability to store charge, which is similar to the function of a capacitor of capacity per unit length $C_M(F/m^2)$. For each of the channels, we know that there will be flux if and only if $V_M \neq E_i$, because E_i, as defined by equation (1.2), represents the equilibrium potential for that particular ion. Therefore we can model each channel as a branch in a circuit with a resistor, which models the irregularities in the channel that oppose the movement of the ions and a generator with a value of E_i.

We then consider three channels, one for sodium, one for potassium and then a final one which takes account of all of the other ions that are not as important, this last one is called the leak (L) channel.

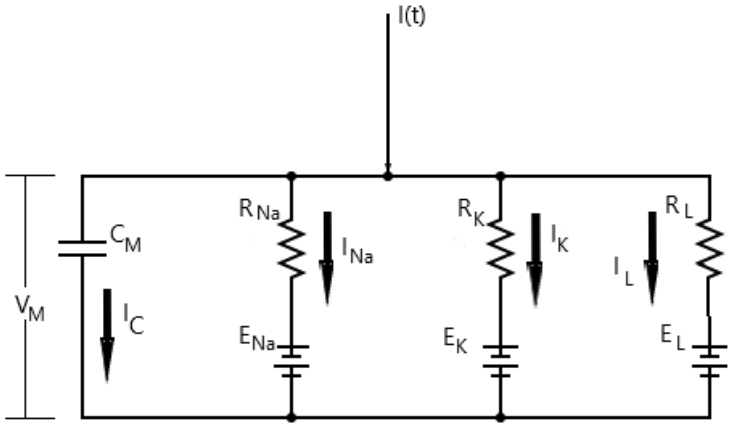

Fig. 3: Equivalent circuit, L stands for "leak".

From the physics of circuits, we know Kirchoff's currents law:

The net sum of the currents entering a node of the circuit is zero.

If we apply this law to the circuit in figure 3, we can see that the current $I(t)$ that is injected in the circuit branches in 4:

$$I(t) = I_C + I_{Na} + I_K + I_L. \tag{5}$$

Which are the currents of the capacitor and the ion channel branches, respectively.

Now, to calculate these currents, we use Kirchoff's voltages law:

The net sum of the voltage drops around a cycle in the circuit is zero.

and Ohm's Law:

$$V = IR,$$

we obtain these expressions:

$$I_C = C_M \frac{dV_M}{dt} \tag{6}$$

$$I_{Na} = \frac{V_M - E_{Na}}{R_{Na}} \tag{7}$$

$$I_K = \frac{V_M - E_K}{R_K} \tag{8}$$

$$I_L = \frac{V_M - E_L}{R_L} \tag{9}$$

where we have used the characteristic equation of a capacitor.

Now, plugging (6), (7), (8) and (9) into (5), we obtain:

$$C_M \frac{dV_M}{dt} = -g_{Na}(V_M - E_{Na}) - g_K(V_M - E_K) - g_L(V_M - E_L) + I(t), \tag{10}$$

where the g_i are the **conductances** per unit length ($S \cdot m^{-2}$) of the channels. These conductances are the inverse of the resistance featured in figure 3.

By defining:

$$g_{tot} = g_{Na} + g_K + g_L$$
$$E_{tot} = g_{Na}E_{Na} + g_K E_K + g_L E_L.$$

We obtain a simpler version:

$$C_M \frac{dV_M}{dt} = -g_{tot}V_M + E_{tot} + I(t). \tag{11}$$

This is an inhomogeneous linear differential equation, which we can easily solve using the variation of constants method obtaining:

$$V_M(t) = V_0 \exp\left(-\frac{t-t_0}{\tau_M}\right) + \frac{E_{tot}}{g_{tot}}\left[1 - \exp\left(-\frac{t-t_0}{\tau_M}\right)\right] + \frac{\exp\left(-\frac{t-t_0}{\tau_M}\right)}{g_{tot}\tau_M}\int_{t_0}^{t} I(s)\exp\left(\frac{s}{\tau_M}\right)ds \tag{12}$$

where $V_0 = V_M(t_0)$ and

$$\tau_M = \frac{C_M}{g_{tot}}$$

is the membrane time constant (s).

If we assume that $V_0 = 0\,V$ we can obtain a much easier equation with which we can make

some simulations to understand the behaviour of the membrane.

From now on, the parameters that we will be using in our simulations will be:

C_M	$1\ \mu F \cdot cm^{-2}$
E_{Na}	$55\ mV$
E_K	-77 mV
E_L	-54.5 mV
g_{Na}	$120\ mS \cdot cm^{-2}$
g_K	$36\ mS \cdot cm^{-2}$
g_L	$0.3\ mS \cdot cm^{-2}$

Table 1: Data used for the numerical experiments involving these constants. Obtained from [2] and [4].

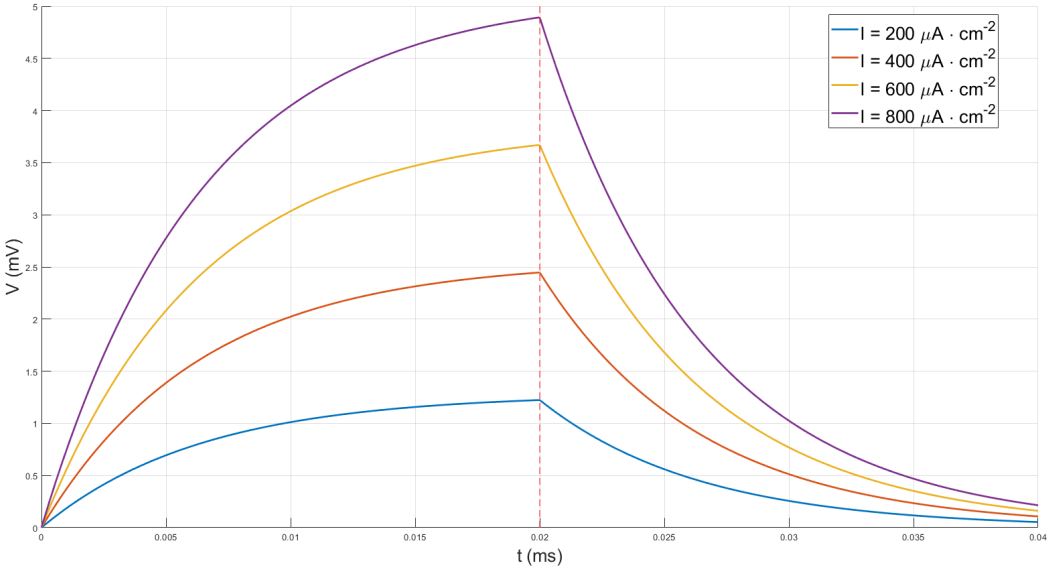

Fig. 4: Voltage response of the neuron following the behaviour described by equation (12) under the stimulus given by a step current starting at $t = 0ms$ and stopping at $t = 20ms$. For these simulations we have used $E_{tot} = 0mV$, $V(0) = 0mV$.

We have to bear in mind that, although we denote current with the letter I, we are really talking about current density or current per unit area ($A \cdot m^{-2}$). The order of magnitude we have used is motivated by the order of magnitude of the other variables in the experiment to achieve a noticeable change in the membrane voltage, but for the moment it is arbitrary.

In this case, although E_{tot} is non-zero, we have decided to set it to zero in order to see the evolution of the voltage with respect to this equilibrium and also because the term corresponding to E_{tot} grows fast enough not to allow us to observe the behaviour of the function.

From the graph, we can see the behaviour described by the equation (12) if the integrand is constant. If we had subjected the system to a constant pulse for an indefinite time, without

neglecting E_{tot} we would obtain:

$$V(\infty) = \frac{E_{tot} + I}{g_{tot}}.$$

As the stable equilibrium of the system.

1.4. Hodgkin-Huxley equations

1.4.1. The Problem with the equivalent circuit

The model we just saw only describes the membrane voltage at a point of its surface but we already know that the neuron has a very elongated part through which this pulse is propagated: the axon.

The axon is a dissipative medium and as such, the signal will eventually be lost. If we consider the axon a linear cable and each point of its surface a circuit like the ones we studied then there is no way that a signal can be sent.

In nature, there are a lot of examples of ondulatory phenomena in dissipative mediums. For example, the case of Domino pieces in a relatively dense fluid, such as water. If the first piece is hit with a force below a given threshold, it will oscillate slightly with respect to its equilibrium position, however, if we hit it with more force, there will be a point at which the piece will lie down and hit the next one, producing a periodic phenomenon.

These phenomena consist of a trigger that fires a periodic effect once getting the value of a variable over a threshold. However, should this threshold not be surpassed, the movement will eventually die out.

The answer to the problem of dissipation in the former section would be given by Hodgkin and Katz, who discovered that the conductances of the ions were in fact non constant. There exist some special types of channels that open whenever the membrane voltage is depolarized above a threshold thus increasing the conductance of that specific ion: **voltage-gated channels**.

1.4.2. Voltage-gated channels

To describe these voltage-gated channels we will follow a probabilistic approach. The conductivity of an ion depends on the number of channels permeable to that ion in a given time. When a channel is closed there is a probability $P_{open}(V_M)$ that it opens and when a channel is open there is a probability of it closing down $P_{close}(V_M)$.

Then let $m \in [0, 1]$ be the fraction of open channels for a selected ion.

The evolution of this fraction of channels is easily given by the following equation:

$$\frac{dm}{dt} = P_{open}(V_M)\,(1 - m) - P_{close}(V_M)\,m. \tag{13}$$

m is the fraction of channels that are open so the only thing they can do is close. $1-m$ is then the fraction of closed channels and therefore they can open with the probability we stated before. These functions are not really probabilities, but, in reality, are probabilities per unit time (s^{-1}) because they represent the probability of opening or closing at an instant of time. They are obtained through experimentation. The name of the probabilities can be misleading due to the fact that they do not sum up to unity. This is because they represent the probability of opening and closing when a channel is already closed or open, respectively. The normalization is given if we sum to each case the probabilities of remaining closed or opened.

This equation, when the voltage is not constant, is not analytically solvable. However, by using **Picard's Theorem** (Theorem 0.6.1) knowing that $f(t,m)$ is Lipschitz with respect to the second variable (this is trivial knowing that the probabilities are bounded and that f is linear), we easily deduce that this equation has a unique local solution for each initial data $m(t_0)=m_0$. We must not forget that V_M has an implicit dependence on time which we do not know.

Before going further, it is important to show the fact that equation (13) can be transformed into:

$$\frac{dm}{dt}=\frac{m_\infty(V_M)-m}{\tau_m(V_M)} \tag{14}$$

where the coefficients are defined by:

$$m_\infty(V_M)=\frac{P_{open}(V_M)}{P_{open}(V_M)+P_{close}(V_M)}, \qquad \tau_m(V_M)=\frac{1}{P_{open}(V_M)+P_{close}(V_M)}.$$

The m_∞ represents the fixed point of the dynamical system (13) and τ_m a time constant which determines the speed of change of that variable. From now on, we will call the X_∞ functions, the **steady-state** of the gating variables.

Lemma 1.4.1. *Given an initial condition $m(t_0)=m_0$ with $0\leqslant m_0\leqslant 1$ and the probability functions are continuous and non-negative, then the equation (13) has a unique solution $\phi_m(t)$ that exists in $[t_0,\infty)$ and $0\leqslant\phi_m(t)\leqslant 1$, $\forall t\in[t_0,\infty)$.*

Proof: If the functions $P_{open}(V_M)$ and $P_{close}(V_M)$ fulfil the conditions in the hypothesis of the Lemma, then we can assure that:

$$0\leqslant m_\infty(V_M)\leqslant 1,\ 0<\tau_m(V_M)<\infty.$$

Now, onto the proof.

We know as we said before, that, given an initial condition, we have a local solution to the differential equation $\phi_m(t)$. That means that the solution will exist in a finite time $[t_0,t_0+\tau)$, $\tau>0$ and we must prove that it will not go to infinity in order for it to be a global solution for all positive times.

By looking at equation (14), we can easily see that the derivative to the left of $m_\infty(V_M)$ is positive and to the right is negative, meaning that it will attract the trajectories:

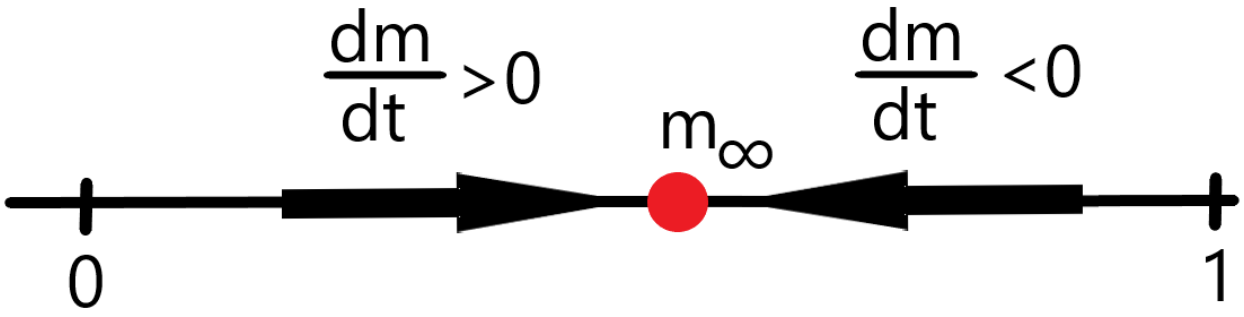

Fig. 5: Behaviour of the derivative at both sides of m_∞.

However, as we do not know anything about the dependence of $V_M(t)$, the only thing we can take from this is the fact that the derivative to the right of 1 is always negative and to the left of zero positive, because the attractive point is always in this interval. Therefore, let us suppose that our function $\phi_m(t)$ goes to infinity in a finite time t^* (the treatment if the function goes to $-\infty$ is analogue and therefore will not be covered). Then, as for one of the hypotheses of this Lemma, we know that at t_0 the function was in the interval $[0, 1]$, and also, as a consequence of Picard's Theorem, the solution is continuous in the interval in which it is defined, namely $[t_0, t^*)$. Therefore, there exists at least an instant of time $t_0 < t' < t^*$ in which the function was 1:

$$\phi_m(t') = 1.$$

If we choose t' to be the last time the function achieves 1 before going to infinity, then, between the times t' and t^*, $\phi_m(t)$ is increasing, which goes against the monotony imposed by equation (14).

□

For the most basic model using Hodgkin and Huxley's formalism, we need three gating variables m, n and h. The functions used by Hodgkin and Huxley in their articles [4] where:

$$P^n_{open}(V) = 0.01\frac{V+55}{1-\exp\left(-\frac{V+55}{10}\right)}, \quad P^n_{close}(V) = 0.125\exp\left(-\frac{V+65}{80}\right),$$

$$P^m_{open}(V) = 0.1\frac{V+40}{1-\exp\left(-\frac{V+40}{10}\right)}, \quad P^m_{close}(V) = 4\exp\left(-\frac{V+65}{18}\right),$$

$$P^h_{open}(V) = 0.07\exp\left(-\frac{V+65}{20}\right), \quad P^h_{close}(V) = \frac{1}{1+\exp\left(-\frac{V+35}{10}\right)}.$$

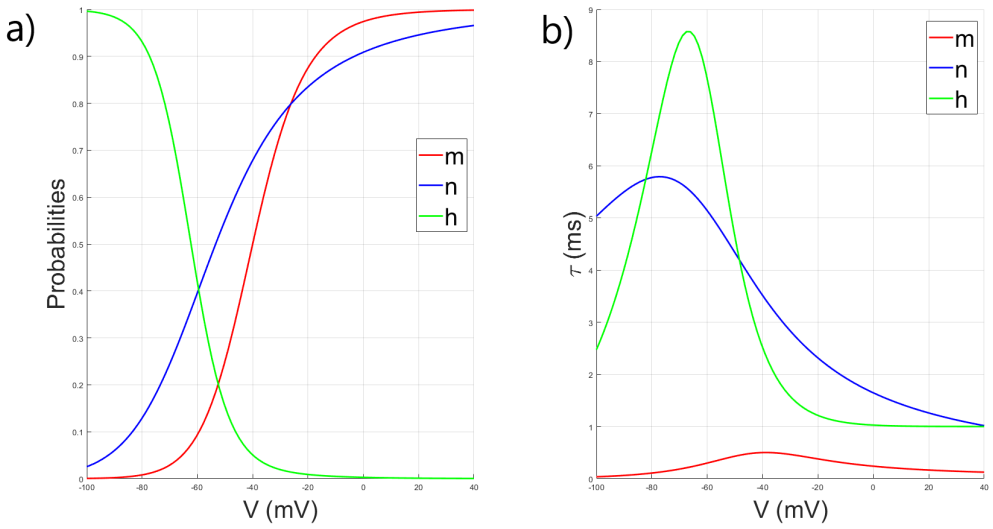

Fig. 6: Evolution of the functions involved in equations (14). **a)** Steady-state of the gating variables. **b)** Time constants of the gating variables.

The input must be expressed in (mV) and the output is in (ms^{-1}). These functions are all continuous and non-negative. This is easily seen for some, but for others, simply applying L'Hôpital's rule allows us to define them at their conflicting points so that they are continuous.

With this Hodgkin and Huxley modelled the variation of the conductances:

$$g_K = \overline{g_K}\, n^4, \qquad\qquad g_{Na} = \overline{g_{Na}}\, m^3\, h. \tag{15}$$

The exponents have biological meaning, the exponent 4 in the potassium is due to the four particles needed to be attached to the membrane to open the gate. The h variable in the sodium gate is an inactivation variable (biologically a blocking particle) and the exponent 3 over the m are the 3 particles needed for the gate to open [4].

1.4.3. Hodgkin-Huxley equations and action potentials

With these gating variables, the circuit equation (10), the equations (14) for m, h and n and (15) we have finally deduced the Hodgkin-Huxley equations:

$$C_M \frac{dV_M}{dt} = -\overline{g_K}\, n^4 (V_M - E_K) - \overline{g_{Na}}\, h\, m^3 (V_M - E_{Na}) - g_L(V_M - E_L) + I(t) \tag{16}$$

$$\frac{dm}{dt} = \frac{m_\infty(V_M) - m}{\tau_m(V_M)} \tag{17}$$

$$\frac{dn}{dt} = \frac{n_\infty(V_M) - n}{\tau_n(V_M)} \tag{18}$$

$$\frac{dh}{dt} = \frac{h_\infty(V_M) - h}{\tau_h(V_M)}. \tag{19}$$

These equations are only valid when, by using techniques which are not important as of now, we attain a homogeneous voltage throughout the cell.

This system of coupled non-linear equations is non-analytically solvable. However, these functions are continuous and have continuous partial derivatives so we can assure that for each initial condition, they have a solution and this solution is unique, we know this because of theorems 0.6.1 and 0.6.2.

Lemma 1.4.2. *Given an initial condition* $\phi(t_0) = (V_0, m_0, n_0, h_0)$ *with* $0 \leqslant m_0, n_0, h_0 \leqslant 1$ *and the steady-states and time constants of the gating variables are bounded, then the equation (13) has a unique solution* $\phi(t) = (\phi_V(t), \phi_m(t), \phi_n(t), \phi_h(t))$ *that exists in* $[t_0, \infty)$ *and* $0 \leqslant \phi_m(t), \phi_n(t), \phi_h(t) \leqslant 1$, $\forall t \in [t_0, \infty)$.

Proof: We must prove now that the solution is defined for each $t \geqslant t_0 = 0$. For this, we must find a bound the positive trajectory of the system.

We know that the solution is bounded in the m, n and h dimensions (Lemma 1.4.1).

Let $\phi(t) = (\phi_V(t), \phi_m(t), \phi_n(t), \phi_h(t))$ the solution of (16) given the initial condition $\phi(t_0) = (V_0, m_0, n_0, h_0)$ then by using the integral formulation of the Cauchy Problem we have:

$$\phi_V(t) = V_0 + \int_{t_0}^{t} (-g_{tot}(s)(\phi_V(s) - E_{tot}(s)) + I(s))ds. \tag{20}$$

Where:

$$g_{tot}(t) = \overline{g_{Na}}\phi_h(t)\phi_m(t)^3 + \overline{g_K}\phi_n(t)^4 + g_L. \tag{21}$$

$$E_{tot}(t) = \frac{E_{Na}\overline{g_{Na}}\phi_h(t)\phi_m(t)^3 + E_K\overline{g_K}\phi_n(t)^4 + E_L g_L}{g_{tot}(t)}. \tag{22}$$

By using what we proved in Lemma 1.4.2 and the fact that $g_{tot}(t) > g_L$, $\forall t$, we know that (21) and (22) are both bounded.

Now we subtract $E_{tot}(t)$ from both sides and apply absolute values to both sides of the equation, obtaining, after some algebra:

$$|\phi_V(t) - E_{tot}(t)| \leqslant |V_0| + |E_{tot}(t)| + \|I\|_\infty (t - t_0) + \int_{t_0}^{t} g_{tot}|\phi_V(s) - E_{tot}(s)|\, ds. \tag{23}$$

Now, let us consider that our solution only stays finite in $[t_0, t^*)$ and therefore in $[t_0, t']$ with $t' = t^* - \epsilon$ and that $I \in L^\infty(\mathbb{R})$, then we can do:

$$|V_0| + |E_{tot}(t)| + \|I\|_\infty (t - t_0) \leqslant M. \tag{24}$$

By applying (24) in (23) we can use Gronwall's Lemma (0.6.1) to obtain:

$$|\phi_V(t) - E_{tot}(t)| \leqslant Me^{\int_{t_0}^{t} g_{tot}(s)ds} \leqslant Me^{(t^*-t_0)\|g_{tot}\|_\infty}. \tag{25}$$

As $g_{tot}(t)$ and $E_{tot}(t)$ are bounded, for each finite time t^*, the trajectory remains bounded and therefore can be extended. This concludes our proof that our solution exists in $[t_0, \infty)$.

□

Looking at the equations and graphs we have already shown above with the steady states and time constants (which are not constants, but we will keep this nomenclature), we can qualitatively analyse what is going to happen before we go into more detail. The stimulus that will allow the neuron's potential to overcome the threshold will be given by the intensity represented either by a current injected by the experimenter or by the action potentials of other neurons arriving via the synapse. If the threshold is not reached, there will be a small depolarisation followed by a re-establishment of the equilibrium potential, corresponding to the fixed point of the unexcited system. However, if the value that allows the potential to fire is reached, what will happen is that the variable m will rapidly go to steady state, due to the fact that τ_m is lower than the other time constants, causing the sodium term to be the most important at first and the membrane to **depolarise** (increase its potential) to values close to the sodium Nernst potential, reducing the term $(V_M - E_{Na})$. By the time this happens, the variable h decreases in value as n increases, giving more importance to the potassium term and causing it to **hyperpolarise** (decrease in potential) to values close to the potassium Nernst potential. Once this occurs, n decreases and the equilibrium state is reached again, with no more action potentials being released until a new stimulus is imposed.

This is summarised in the following picture:

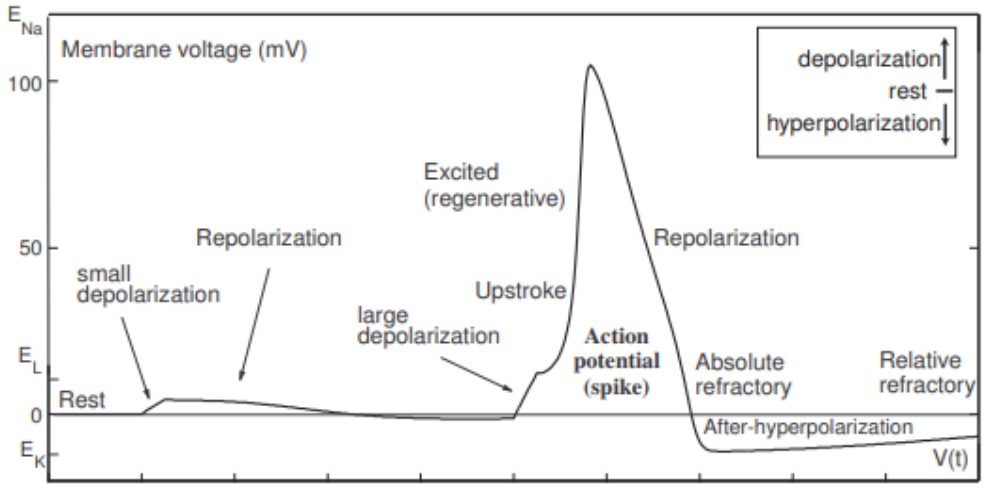

Fig. 7: Action potential explained by means of the dynamical Hodgkin-Huxley system [5].

1.4.4. Quick detour: Hopf bifurcations

We will study the behaviour of the dynamical system of Hodgkin and Huxley by using elements from the qualitative theory of differential equations, mainly Theorem 0.6.3. However, there is something, which is not studied in preliminary courses of differential equations which must be discussed before going further and that is **theory of structural stability**.

If we have a dynamical system dependent on a parameter, as is our case here with I (we will ignore the variability with respect to Nernst conductances and voltages), it is possible that the behaviour of some equilibria or limit cycles of the system changes according to the value of this parameter, i.e. the system does not remain **structurally stable**.

This is what is behind action potentials, which are periodic phenomena generated by the approach of a trajectory to a closed orbit that will act as a limit cycle. These potentials do not occur for any value of the parameter I, but for those in which the conditions are conducive to what we have just explained.

First of all, I would like to mention that the phenomena we will be studying will arise from the change in the local behaviour of the fixed points of the system and that we can infer this behaviour using the linear version of our dynamical system in the vicinity of these points thanks to the following Theorem [6]:

Theorem 1.4.1 (Hartman-Grobman Theorem)**.** *In a vicinity of a hyperbolic fixed point, a dynamical system and its linearized version are topologically equivalent.*

The definition of hyperbolic fixed points is stated in the appendix (0.6.1).

Without entering into much detail about what it means to be topologically equivalent, we will say that two dynamical systems are topologically equivalent when you can find a continuous function that maps trajectories from one system to the other.

The bifurcation with which we will be working in this chapter will be the **Hopf bifurcation** which occurs when two complex eigenvalues of the Jacobian matrix of the system cross the imaginary axis and a fixed point changes from being stable to unstable or vice versa.

Hopf bifurcations come in two flavours: **subcritical** and **supercritical**.

In subcritical bifurcations, there is a point before the bifurcation when an unstable limit cycle and a stable one, both of them around a stable equilibrium, appear. Therefore, trajectories starting between the two cycles will become periodical and the ones starting inside the unstable limit cycle will eventually end at the fixed point. When the threshold is surpassed the unstable limit cycle and the fixed point fuse, making the latter unstable and generating oscillating orbits. These systems present hysteresis, because after lowering the parameter below the Hopf bifurcation, oscillations may not stop until achieving the point we talked about before where the two cycles appear.

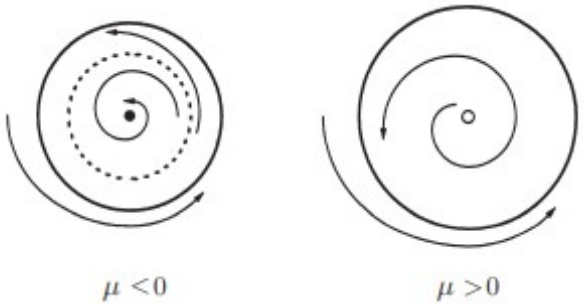

Fig. 8: Behaviour of a subcritical Hopf bifurcation generated by the parameter μ. The unstable limit cycle is represented with the dashed line which we see disappearing and turning the point unstable (white) as $\mu > 0$ [3].

In supercritical bifurcations, the oscillations occur little by little after the threshold is surpassed. The stability is lost as from the point appears a stable limit cycle.

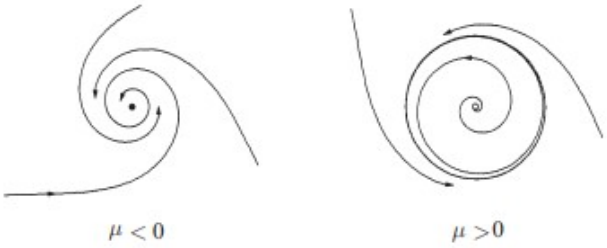

Fig. 9: Behaviour of a supercritical Hopf bifurcation generated by the parameter μ. A stable limit cycle appears as $\mu > 0$ [3].

1.4.5. Fixed Points, Limit cycles and Bifurcations

We will consider $I(t)$ as a constant input and study the **fixed points** depending on its value. By equating Hodgkin-Huxley equations to zero, we obtain that the fixed points will be the solutions to the equation:

$$I = \overline{g_K} n_\infty(V_M)^4(V_M - E_K) + \overline{g_{Na}} h_\infty(V_M) m_\infty(V_M)^3(V_M - E_{Na}) + g_L(V_M - E_L) = F(V_M). \quad (26)$$

So the problem is now simplified, as it only consists in analyzing the number of zeros that the function F has. We have omitted the C_M because in the units we are using its value as 1.

We will be using the data from table 1 for our simulations, as the derivative of (26) will be difficult to discuss analytically, I have done a numerical experiment with MATLAB which shows that the function is monotone. It is also easy to see that the function is surjective and therefore we have a unique solution for each I, which we will call $V_M^*(I)$ from now on.

We now must analyze the local stability of the system by linearizing it and studying the sign of its eigenvalues. The jacobian matrix of the system of Hodgkin and Huxley has the following

form:

$$J(V_M^*(I)) = \begin{pmatrix} -\frac{\partial F}{\partial V} & -\frac{\partial F}{\partial m} & -\frac{\partial F}{\partial n} & -\frac{\partial F}{\partial h} \\ \frac{m'_\infty}{\tau_m} & \frac{1}{\tau_m} & 0 & 0 \\ \frac{n'_\infty}{\tau_n} & 0 & \frac{1}{\tau_n} & 0 \\ \frac{h'_\infty}{\tau_h} & 0 & 0 & \frac{1}{\tau_h} \end{pmatrix} \tag{27}$$

the analysis of the sign of the eigenvalues of the matrix (27) can easily be done numerically (which we will soon be doing) but an in-depth analysis requires a lot of mathematical tools which we will not show. However in [7], Troy shows that there exist two Hopf bifurcations in the system depending on I. We can show this numerically in a graph:

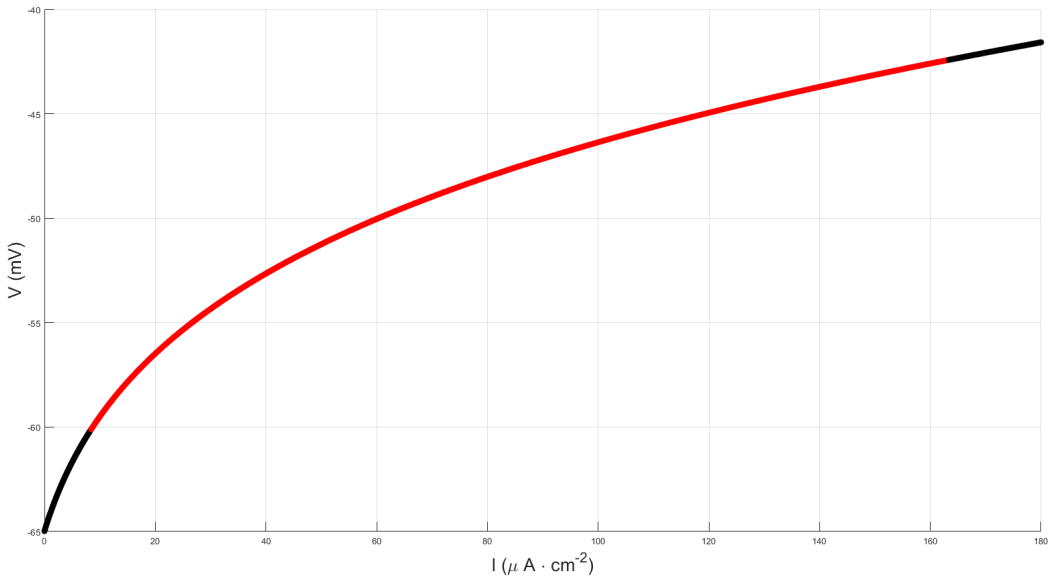

Fig. 10: Evolution of the local stability of the fixed point of Hodgkin-Huxley equations. We represent the value $V_M^*(I)$ as a function of I. Red points are unstable and black points are stable.

Our estimations locate the two bifurcations at:

$$I^1_{Hopf} = 8.44\mu A \cdot cm^{-2}, \qquad I^2_{Hopf} \approx 163.37\mu A \cdot cm^{-2}$$

1.4.6. Numerical Simulations

Now, with the simulations. We start at equilibrium with $I = 0$. ($V(0) = -64.98mV$, $m(0) = 0.05$, $n(0) = 0.32$, $h(0) = 0.60$). First of all, we will use short current pulses which imitate the behaviour of a Dirac delta function:

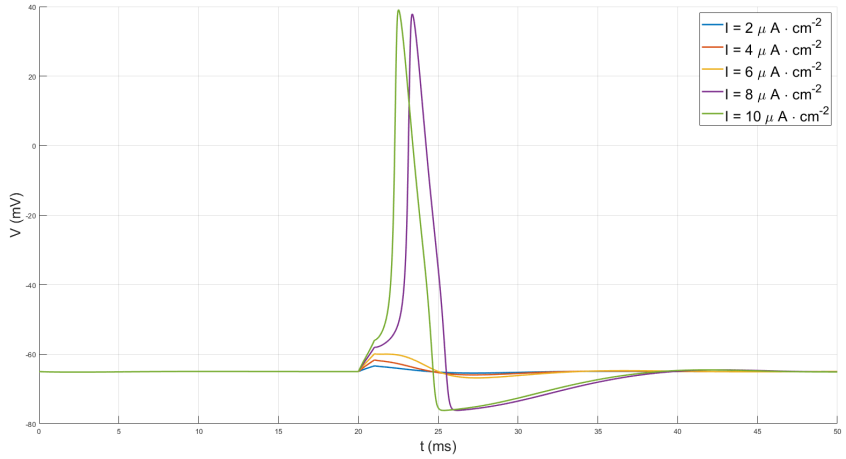

Fig. 11: Response of a neuron predicted by the H-H equations under a Dirac delta-like input fired at 20 ms.

As we see, the action potential is an 'all of nothing' phenomenon, as we had explained before. The threshold we have calculated before is not valid in this type of pulse because it is very sensitive to their duration.

We can understand these Dirac delta pulses as finite and instantaneous jumps in coordinates in the 4D phase plane. When the jump is big enough, the flow of the system starts an action potential which then finishes in the stable equilibrium we calculated before.

Now, if we consider a constant current with greater amplitude than the one we found as the trigger in the latter section, we obtain the following behaviour of the different variables:

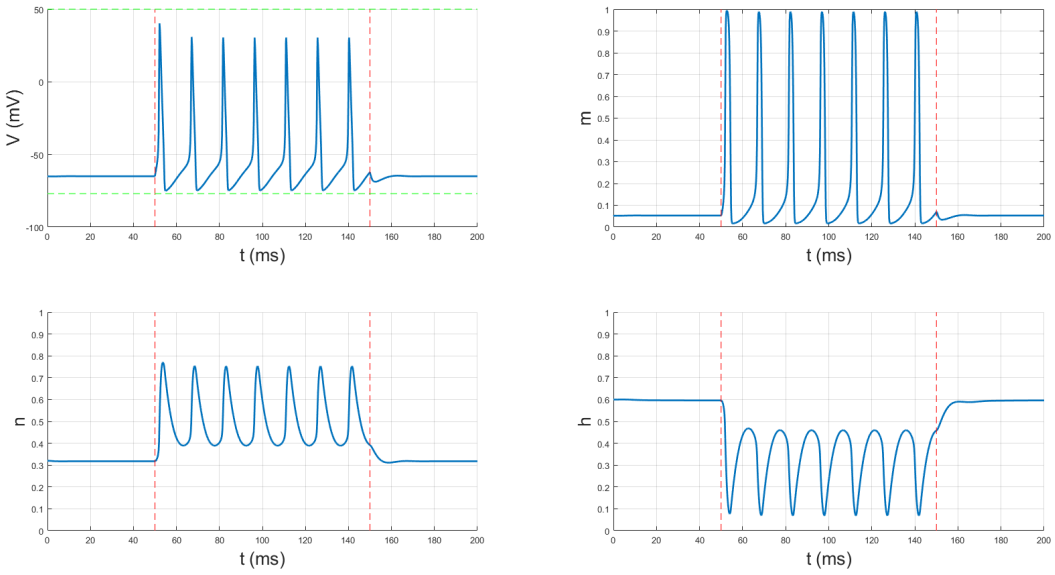

Fig. 12: Response of a neuron predicted by the H-H equations under a step current injected and stopping at the times marked by the red lines. $I = 10\mu A \cdot cm^{-2}$.

We observe repetitive firing, something which is known as **bursting** in the world of neuroscience.

The behaviour that we expected is what we actually see, the first gating variable to fire is the m one whose peaks are narrower than the others because of the smaller magnitude of its gating variable. Also, I have marked with green dashed lines the Nernst potentials of sodium and potassium and we see how it approaches both but it comes nearer the potassium one ($\sim$ -77 mV). When the step current is stopped, the system swiftly approaches rest.

The shape of the peaks of the n and h gating variables is interesting because we see that one is almost the exact opposite of the other, we will make use of this fact in the following chapter to reduce the dimension of the HH system.

Another thing that comes to your mind when seeing this picture is that the first action potential is much higher than the rest, this is due to the solution approaching the limit cycle in spiral motion. This can be easily observed in figure 13:

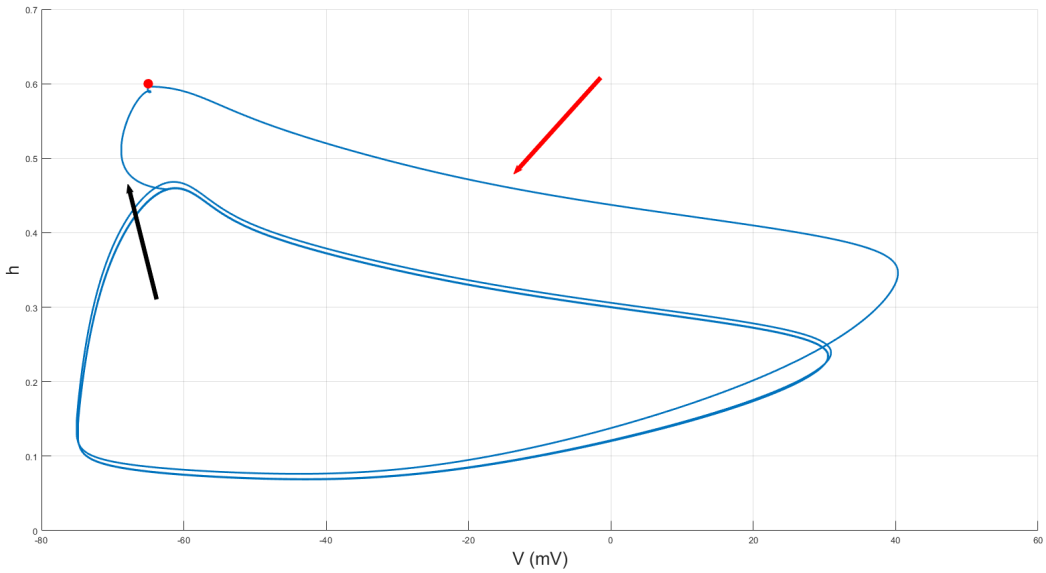

Fig. 13: Phase-plane portrait of the former situation. The red point is the start of the orbit.

The black arrow signals the first action potential as it approaches the limit cycle and the red arrow the return to the initial state of rest after firing 7 times (doing 7 turns).

This is proof of the usefulness of this model because this is something that is actually observed in neurons when they fire several action potentials, which is the bursting we mentioned before.

Now, we can calculate the frequency of these action potentials as a function of I, as it is characteristic of the type of model that we have, as we will see later, which gives us the following graph:

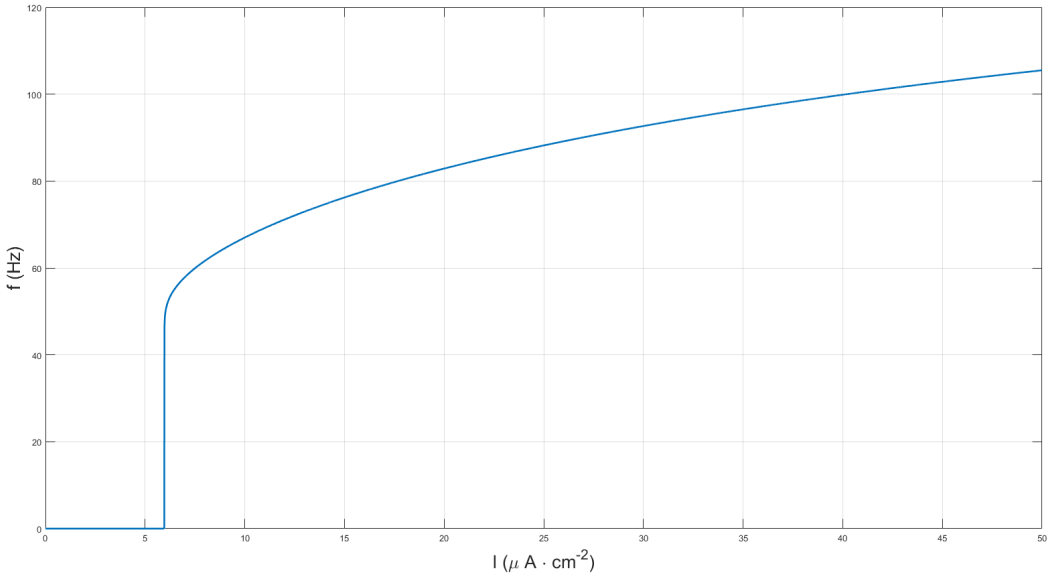

Fig. 14: $f - I$ graph for a H-H neuron.

Due to the computational difficulty of calculating these graphs, we cut before the second bifurcation occurs. The important detail of this one is the discontinuity that occurs near the first bifurcation, which we will see is characteristic of Hopf-type bifurcations. The fact that oscillations begin before the value of the bifurcation is a hint that maybe we have a subcritical Hopf bifurcation.

We can do a little numerical experiment to see another hint that the first bifurcation may be subcritical. We will model the intensity as a decreasing ramp and this is what we observe:

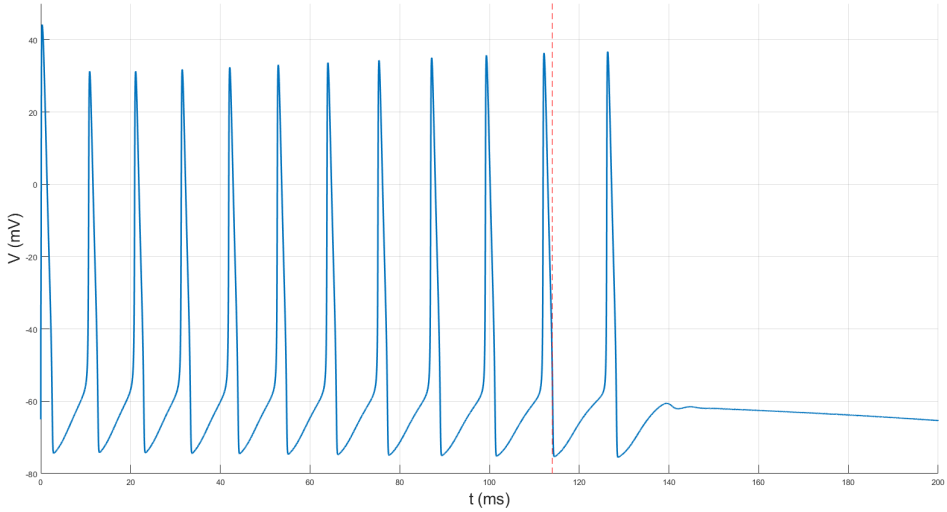

Fig. 15: Response of the HH equations under an input $I(t) = 20 - 0.1 \cdot t\, \mu A \cdot cm^{-2}$. The red dashed line indicates the point at which $I(t)$ equals the bifurcation value.

The hysteric behaviour is typical of subcritical Hopf bifurcations. However, this is by no means a rigorous proof, even though the literature tells us that it is in fact, subcritical [2], [7].

For the second bifurcation, we can show that the amplitude of the oscillations begins to decline long before it is surpassed:

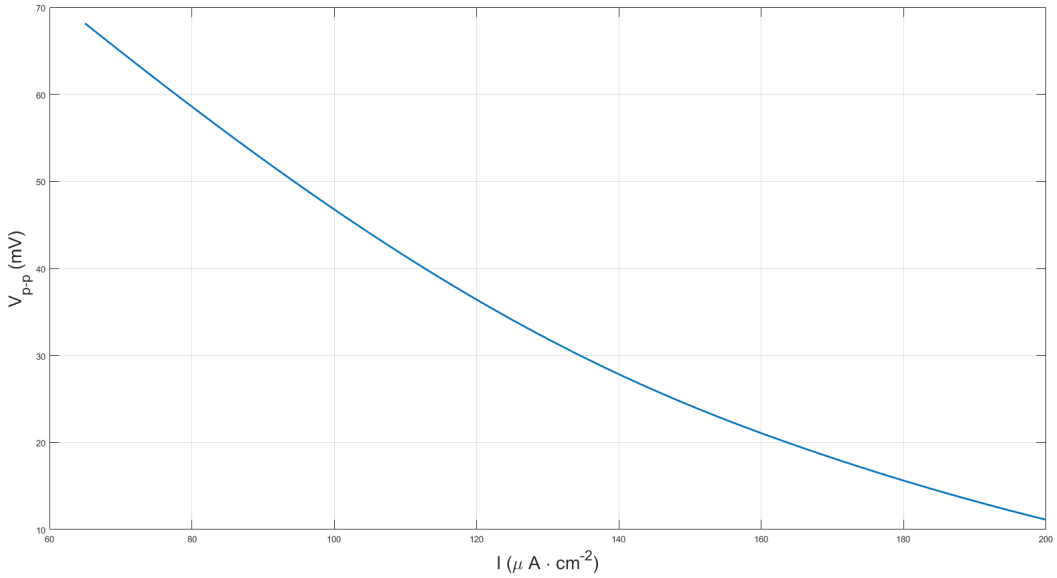

Fig. 16: Peak to peak voltage of the signals as a function of the applied intensity.

Therefore, it seems that this second bifurcation is supercritical.

All in all, we have successfully obtained the Hodgkin-Huxley equations, the most fundamental differential system in neuroscience. It is worth saying that we can extend this system to include the influence of each one of the channels that are present in a cell's membrane. However, this will increase notably the computational effort to calculate the solutions.

Chapter 2: Reduction to a 2D model

2.1. Simplifications of the Hodgkin-Huxley model

Let us consider the differential system that we obtained in the former chapter:

$$\begin{aligned} C_M \frac{dV_M}{dt} &= -\overline{g_K}\, n^4 (V_M - E_K) - \overline{g_{Na}}\, h\, m^3 (V_M - E_{Na}) - g_L(V_M - E_L) + I(t) \\ \frac{dm}{dt} &= \frac{m_\infty(V_M) - m}{\tau_m(V_M)} \\ \frac{dn}{dt} &= \frac{n_\infty(V_M) - n}{\tau_n(V_M)} \\ \frac{dh}{dt} &= \frac{h_\infty(V_M) - h}{\tau_h(V_M)}. \end{aligned}$$

There are two tools that will help us reduce the dimensionality of the system. The first one is the separation of timescales. We have seen in figure 6 that $\tau_m \leqslant \tau_h$ and that $\tau_m \leqslant \tau_n$, the m variable is much faster than the other two. Therefore, we can assume that the m gating variable arrives at the value $m_\infty(V_M(t))$ instantly. The other tool that we can use is the relationship that exists between h and n, which we can see in figure 12. We can see that their behaviour can be related linearly:

$$w(t) = b - h(t) = an(t) \tag{28}$$

with a and b positive constants.

Therefore, we can write a new system of equations:

$$\begin{aligned} C_M \frac{dV_M}{dt} &= -\overline{g_K} \left(\frac{w(t)}{a}\right)^4 (V_M - E_K) - \overline{g_{Na}}\, (b - w(t))\, m_\infty^3(V_M)\, (V_M - E_{Na}) - g_L(V_M - E_L) + I(t) \\ \frac{dw}{dt} &= \frac{w_\infty(V_M) - w}{\tau_w(V_M)}. \end{aligned}$$

The uniqueness and the global existence of the solution of these equations is a corollary of Lemma 1.4.2.

More numerical experiments confirm that there is a unique fixed point for each I and the arguments from [7] can be also applied to this situation to confirm the existence of two Hopf bifurcations.

2.1.1. Simulations

Using the data from table 1, we can adjust points from a simulation of HH equations at, let us say $I = 10\mu A \cdot cm^{-2}$, to obtain values for the parameters.

We have used a lot of data for the parameters and plotting the points can be a bit confusing, but the fact, that they approach the line so closely and that its monotony is the one predicted

by (28) makes us confident of our estimation:

$$a = 1.0939, \qquad b = 0.8949$$

We can see here how the "experimental" points adjust to a line:

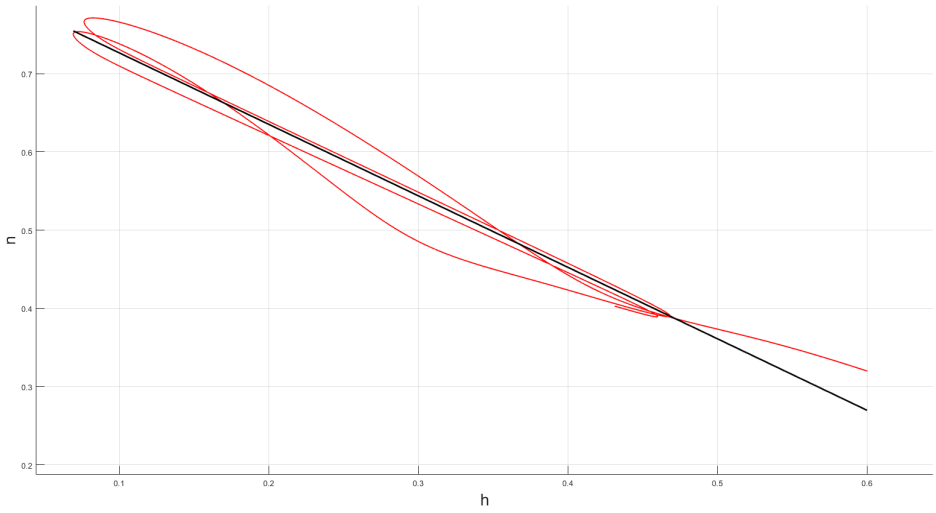

Fig. 17: Linear regression used to obtain the parameters for the HH simplified model. In red the data and in black the adjusted line.

With this data, we do the following simulation:

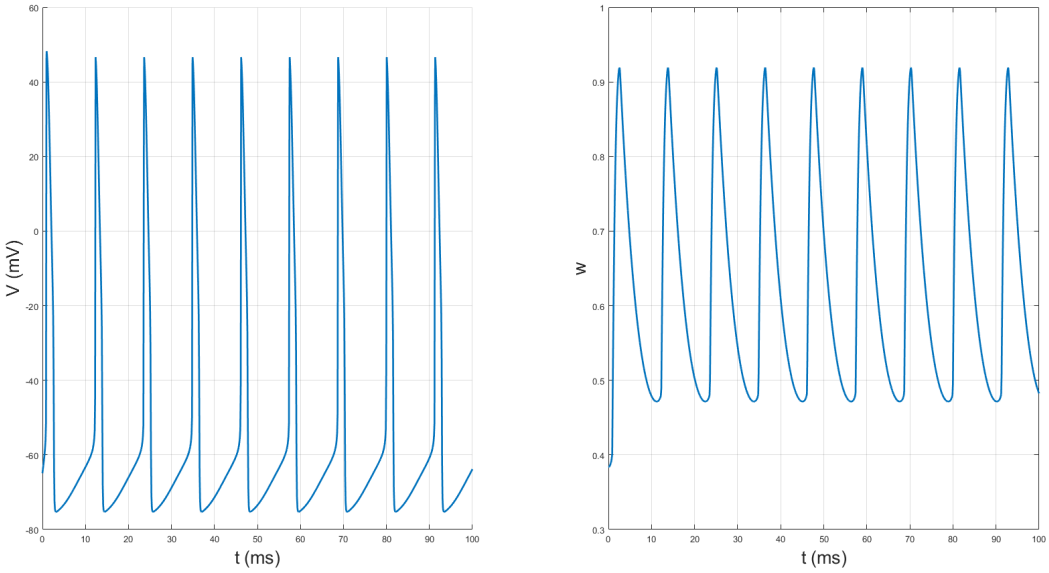

Fig. 18: Simulation of the HH simplified equations under a constant current of I = 10 $\mu A \cdot cm^{-2}$.

As we have seen the behaviour of this system in 4D, we will analyze a different model in detail in this chapter, showing the potential of phase-plane analysis.

2.2. The $I_{Na,p} + I_K$ model

The Hodgkin-Huxley reduced model shows us, like in the case of its 4D version, how oscillations can be produced when a pair of complex conjugates eigenvalues cross the imaginary axis, which is what we called the Hopf Bifurcation. However, this is not the only mechanism that can produce limit cycles nor the Hopf Bifurcation is the only type of structural change that a system can suffer. Now, we will propose a very similar model that hides another type of change in its fixed point, the $I_{Na,p} + I_K$ model [5]:

$$\begin{aligned} C_M \frac{dV_M}{dt} &= I - g_L(V_M - E_L) - g_{Na} m_\infty(V_M)(V_M - E_{Na}) - g_K w(V_M - E_K) \\ \frac{dw}{dt} &= \frac{w_\infty(V_M) - w}{\tau_w(V_M)}. \end{aligned}$$

In this model, the sodium current is persistent due to the fact that we have removed the closing of the gates by the $1 - w$ variable, from this fact comes the p in the name of the model. Also, we have changed the potassium current so that it can activate way faster because now the exponent in the potassium gating variable (in this case w) is 1.

Again, this model has not an analytical solution but the regularity and the linearity in V_M in the first equation allow us to resort to proofs made in the former chapter to assure the global existence and uniqueness of the solutions of this system for each initial condition.

For this model, the simulations and the analysis will be more visible, because we will use graphic tools that we couldn't before because of the higher dimensionality of the space.

The data for these simulations will be slightly different than the one we used before and it is summarised in the following table:

C_M	1 $\mu F \cdot cm^{-2}$
g_L	8 $mS \cdot cm^{-2}$
g_{Na}	20 $mS \cdot cm^{-2}$
g_K	10 $mS \cdot cm^{-2}$
E_L	- 80 mV
E_{Na}	60 mV
E_L	-80 mV

Table 2: Data for the simulations of the $I_{Na,p} + I_K$ model.

And the steady-states and time constants:

$$m_\infty(V_M) = \frac{1}{1+\exp\left(-\dfrac{V+20}{15}\right)},$$
$$w_\infty(V_M) = \frac{1}{1+\exp\left(-\dfrac{V+25)}{5}\right)},$$
$$\tau_w(V_M) = 1.$$

First, we should see the nullclines and their intersections when $I = 0$:

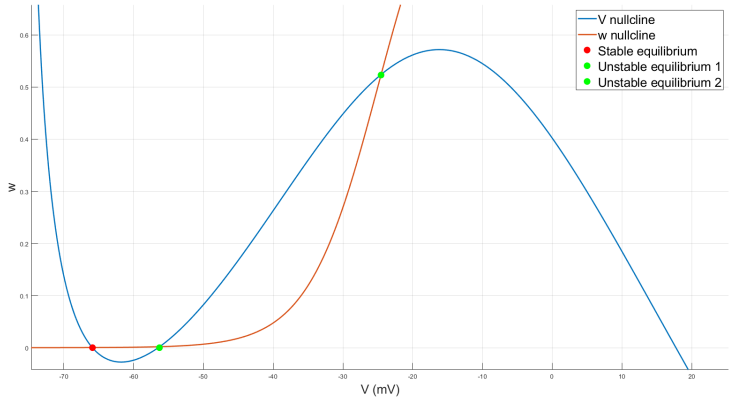

Fig. 19: Nullclines of the differential system for $I = 0$. In red is the stable equilibrium and in green the unstable equilibria.

The intersection of $w_\infty(V_M)$ (w-nullcline) and the V_M-nulcline consists of three fixed points for this value of I. The one to the left is stable and the other two are unstable. However, the second one is what we call a **saddle point** which is a fixed point whose eigenvalues have different signs, which makes them approachable in a specific direction, the one given by the eigenvector corresponding to the negative eigenvalue.

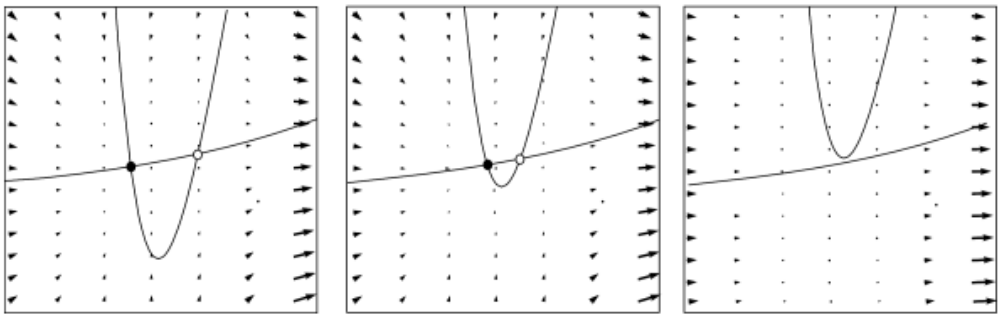

Fig. 20: The process by which two points, one stable and another a saddle point, merge into a saddle-node [8].

When considering the differential system, it is noticeable that the only nullcline whose location and shape will be affected by the change in the parameter I is the V_M-nulcline which will raise. This will not change the stability of the fixed points but the two points to the left will start approaching until merging in one like what is shown in figure 20, this new point is called a **saddle-node** and has the properties of a saddle point. If we further increase the current, the points disappear and a **Saddle-node bifurcation** happens.

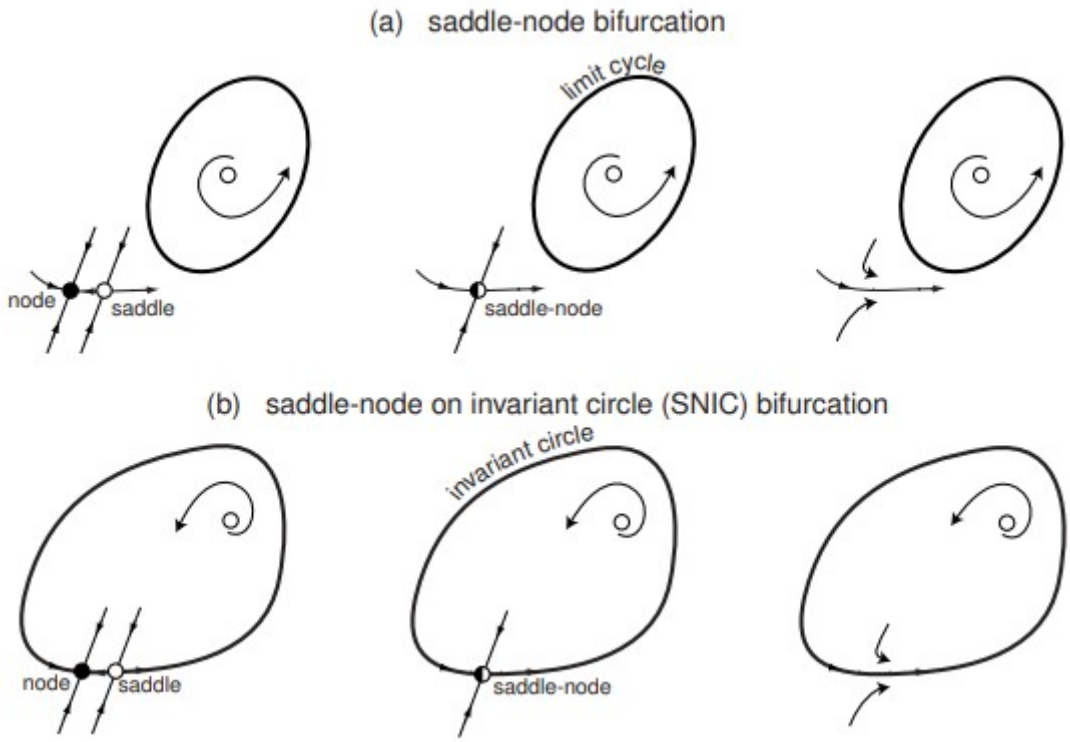

Fig. 21: Different types of saddle-node bifurcations [5].

What happens in the case of Hopf bifurcations happens also with saddle-node bifurcations. As we can see in figure 21, there are two kinds, one that ignores the former saddle-point altogether and the saddle-point-on-invariant-cycle (SNIC) bifurcation, which is the one we seem to have based on the experiments that we will be doing in the near future. In this type of saddle-node bifurcations, the "ghost" of the former fixed points bends the trajectories and attracts them.

We can obtain an estimate for the bifurcation point:

$$I_{SNIC} = 4.40\mu A \cdot cm^{-2}.$$

Similarly to what we did with the Hodgkin-Huxley equations, we can plot the evolution of the coordinates of the fixed points and their local stability depending on the value of the intensity applied and obtain:

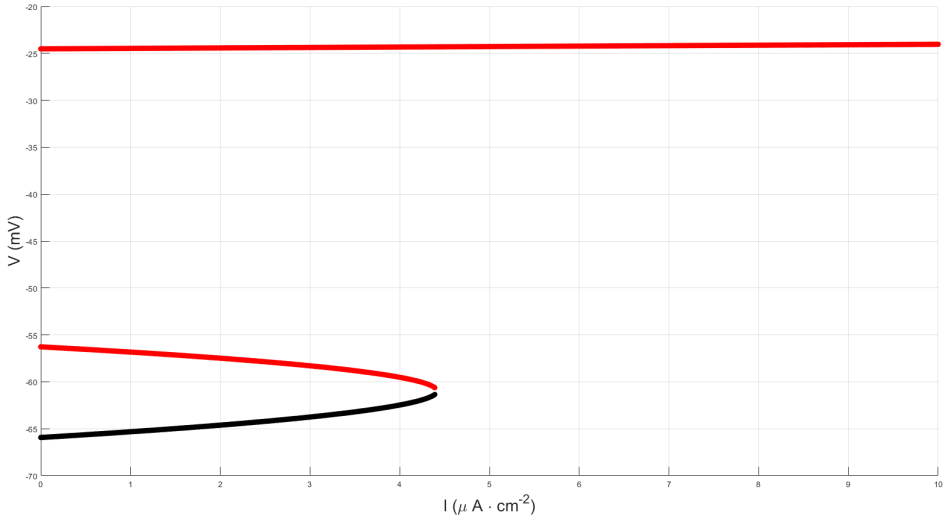

Fig. 22: Evolution of the local stability of the fixed points depending on the current injected. In red the unstable points and in black the stable ones.

Due to the non-linearity of the $w - nulcline$ is not a good option, but we could obtain another estimate for the intensity at which the bifurcation happens using geometry and the fact that, when the two points merge, the tangent line to both curves is the same.

If we raise the current above the threshold we have just calculated, we observe repetitive firing:

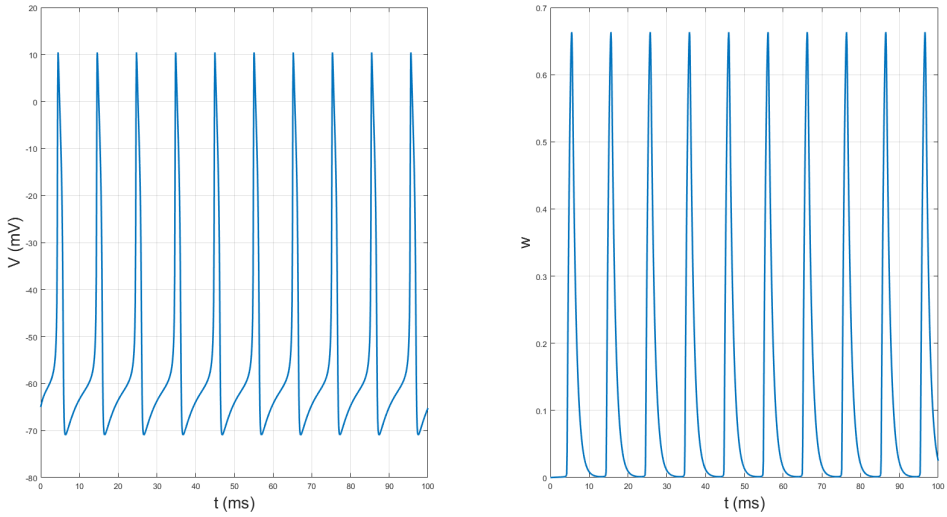

Fig. 23: Periodic firing generated by the $I_{Na,p} - I_K$ model with I $= 6\ \mu A \cdot cm^{-2}$.

Repetitive firing as a consequence of falling into a limit cycle whose existence can be proven easily using Theorem 0.6.4.

The fact that this limit cycle passes near the point where the saddle-node was is the hint I

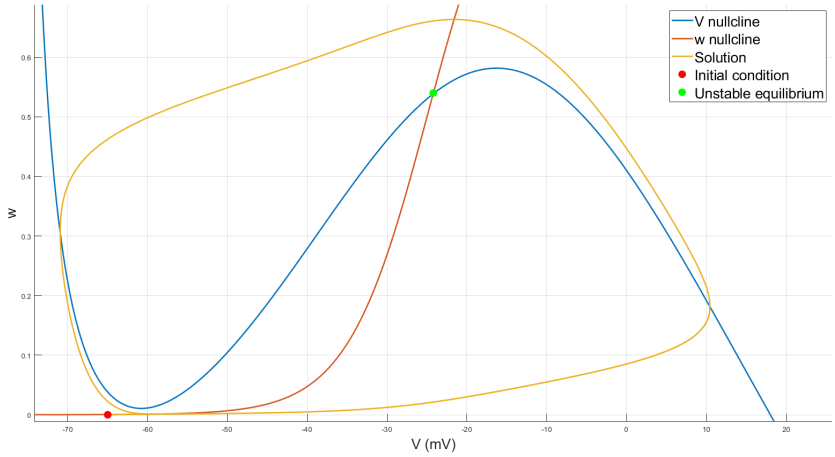

Fig. 24: Limit cycle that generates the periodic firing in the $I_{Na,p} - I_K$ model with I = 6 $\mu A \cdot cm^{-2}$.

talked about before when we guessed that we are experiencing a SNIC bifurcation.

We can see the $f - I$ diagram of these neurons and we find something interesting:

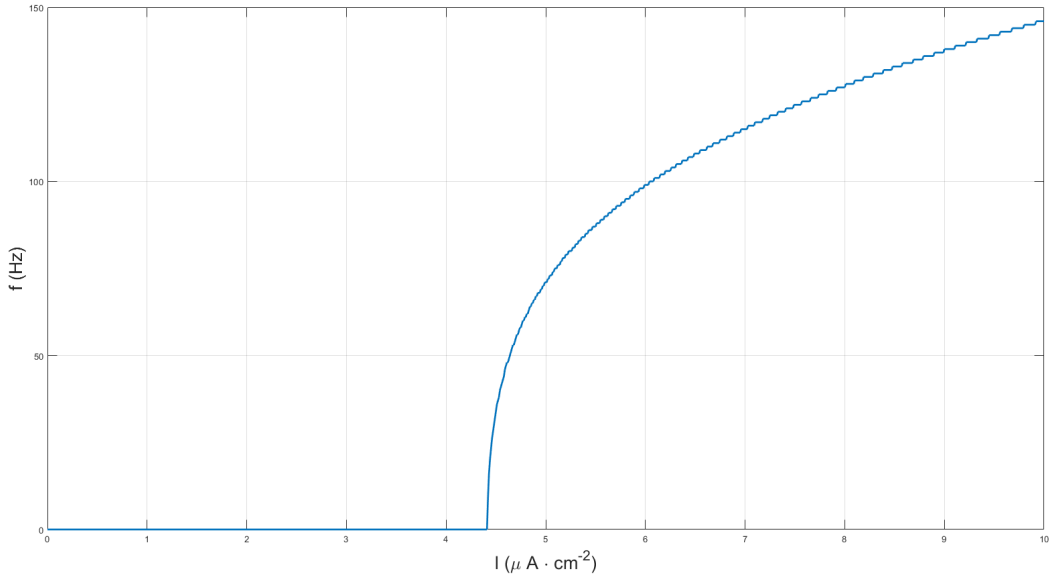

Fig. 25: $f - I$ graph for a $I_{Na,p} - I_K$ neuron. Results have been recorded over a 1s pulse.

In this case, we do not observe a discontinuity, this is a consequence of the internal workings of a saddle-node bifurcation, where the frequency dependency is proportional to $\sqrt{I - I_{SNIC}}$. In the next chapter, we will work with another model that shows the same behaviour and obtain this relation for every model that has the same type of bifurcation.

The fact that the frequency starts from 0 and is continuous makes it possible to adjust the distance between subsequent action potentials.

2.3. Class I and Class II

We have seen two types of behaviours in the $f - I$ characteristic of our models, these were categorised by Hodgkin in two different classes:

- **Class I:** They can start firing at arbitrarily low frequencies and the time between peaks is short.
- **Class II:** They have a discontinuity in their $f - I$ graph and the recovery time between peaks is longer.

Neurons that do not belong to any of these two groups are viewed as abnormal. The remarkable thing is that the shape of these curves depends on the type of bifurcation that serves as a threshold for their action potentials: models with Hopf bifurcations generate class II graphs while models with Saddle-node bifurcations generate class I $f - I$ characteristics.

Neurons of different parts of the brain behave in one way or another, this classification is exhaustive as neurons that do not correspond to either of the categories are considered anomalous.

Chapter 3: 1D models

In this chapter, we will be studying 1-dimensional models specifically designed for their application in neural networks. We will start from the famous Leaky Integrate-and-fire model and conclude with the ring models used for neurons in the visual cortex.

3.1. Further simplification of the Hodgkin-Huxley system

In the former chapter, we studied two models whose orbits follow the dynamics given by systems of equations of the form:

$$\tau_M \frac{dV_M}{dt} = F(V_M, w) + R_M I(t)$$
$$\tau_w \frac{dw}{dt} = G(V_M, w)$$

where $\tau_M = R_M C_M$. In the actual experience, it is usually seen that $\tau_w >> \tau_M$ and thus the derivatives in the phase plane are almost horizontal. Therefore it is entirely justified to suppress the second equation and obtain the following:

$$\tau_M \frac{dV_M}{dt} = F(V_M) + R_M I(t). \tag{29}$$

This is the general equation of **Integrate-and-fire** models. It is obvious that a local solution given an initial condition $V(t_0) = V_0$ exists and is unique if F is sufficiently regular, which will be the case in the following cases.

Before starting the analysis of the models, from now on we will not give too much importance to the units of the magnitudes because, in this type of model, abstractions are used that go beyond the concrete physics of the models. This will not be a big problem since units have not played an important role up to now.

3.2. Leaky Integrate-and-fire

The leaky integrate-and-fire is a very simple model in which the F function in equation (29) is a linear one:

$$\tau_M \frac{dV_M}{dt} = -(V_M - V_{rest}) + R_M I(t). \tag{30}$$

This equation is obtained through a circuit like the one in (10) but with only one channel with resistance R_M and then $\tau = R_M C_M$. This model is called leaky because we see that the only current that we consider is the "leak" one, the one with constant conductance. We can

easily find a general solution given an initial condition $V(t_0) = V_0$:

$$V_M(t) = V_0 \exp\left(-\frac{t-t_0}{\tau_M}\right) + V_{rest}\left[1 - \exp\left(-\frac{t-t_0}{\tau_M}\right)\right] + \frac{\exp\left(-\frac{t}{\tau_M}\right)}{C_M}\int_{t_0}^{t} I(s)\exp\left(\frac{s}{\tau_M}\right)ds. \tag{31}$$

This system has the same response that we saw in the first chapter when we approximated the membrane by an equivalent circuit. The interesting thing that these models do and why they are useful is that they serve us to sum (integrate) the inputs that other neurons send when they fire an action potential, modulated by the Green function of the system which is, in this case, $\exp\left(\frac{s}{\tau}\right)$.

The fact is that, as we had seen with the equivalent circuit in Chapter 1, this is not the behaviour we want. With this model let alone like this we will not observe repetitive firing. It only has a fixed point which is always attractive as the Jacobian of the system is always -1, therefore all of the trajectories will be attracted to it.

The solution to this problem is to insert a manual threshold. If the membrane potential arrives at a value V_{th}, then it is reset manually in $V_{reset} < V_{th}$ after waiting a time which we call the **refractary time** t_{ref}, analogue to the one we saw in actual action potentials.

For the sake of simplicity and mathematical cleanliness, we will only consider the cases such that $V_{reset} = V_R$ and $t_{ref} = 0$.

This gives us the following properties for the model:

Property 3.2.1. *When considering a constant current input $I(t) = I$, the system has a current threshold for firing given by the expression:*

$$I_{min} = \frac{V_{th} - V_R}{R_M}.$$

Proof: Let us consider a constant current to determine the threshold.

The steady state of the system is given by:

$$0 = -(V(\infty) - V_R) + R_M I. \tag{32}$$

For a system to fire, the membrane potential must arrive at V_{th}, the most extreme case is that the system arrives at this threshold at infinity, therefore, substituting $V(\infty)$ with V_{th} in (32) we obtain the result. □

Property 3.2.2. *If $V_0 = V_R$, the frequency of firing is given by the equation*

$$f = \frac{1}{\tau_M \ln\left(1 + \frac{I_{min}}{I - I_{min}}\right)}, \tag{33}$$

which behaves linearly at high currents.

Proof: If the current is constant and $V_M(0) = V_0 = V_R$, the equation (31) turns into

$$V(t) = V_R + R_M I(1 - e^{-\frac{t}{\tau_M}}),$$

because $t_{ref} = 0$ and $V_{reset} = V_R$, we know that the period of the signal is the time that it takes for it to go from the reset to the threshold and can be thus calculated:

$$V_{th} = V_R + R_M I(1 - e^{-\frac{T}{\tau_M}})$$

where, doing some algebra and using Property 1, we obtain:

$$f = \frac{1}{T} = \frac{1}{\tau_M \ln\left(1 + \frac{I_{min}}{I - I_{min}}\right)}.$$

Then, for $I >> 1$, we can use the Taylor expansion of the logarithm:

$$\ln(1 + x) = x + o(x).$$

And we obtain:

$$f_{I>>1} \approx \frac{I - I_{min}}{\tau_M I_{min}}$$

which is linear.

□

Corollary 3.2.1. The LIF model is class I.

Using the following data:

R_M	0.125 $k\Omega$
τ_M	0.125 ms
V_R	-65 mV
V_{th}	40 mV

Table 3: Data for the simulations with the Leaky Integrate-and-fire model.

Using the formula given by equation (3.2.1), we can estimate the value of the minimum current with these parameters:

$$I_{min} = 840\mu A.$$

We can do a simple simulation to show the behaviour of the model:

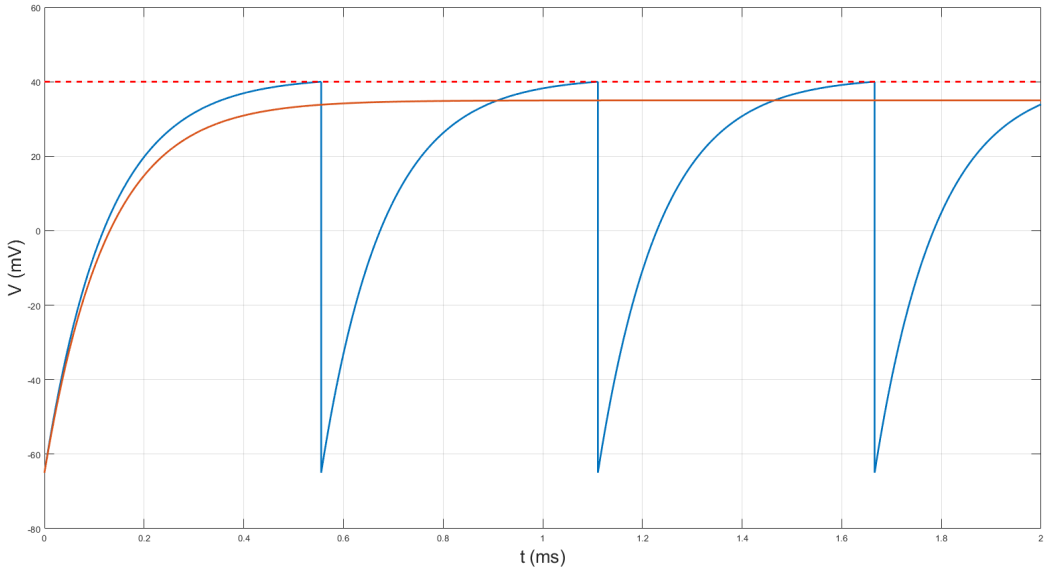

Fig. 26: Simulation of the Leaky Integrate-and-fire model under a constant current stimulus. In orange if $I < I_{min}$ and in blue $I > I_{min}$. The red dashed line indicates the position of the threshold.

When the current is not smaller than the threshold ($I_{min} = 840\mu A$) the system does not fire, as predicted, but when it is greater, the repetitive firing cannot be stopped.

In terms of the phase space (or in this case phase-line), it is easy to see why this happens. The steady-state if $I > I_{min}$ will be over V_{th} and, as we said before, will be attractive. When the points approach the equilibrium but surpass the threshold, the system sends the trajectory back to the starting point.[1]

3.3. Quadratic Integrate-and-Fire

The function $F(V_M)$ which appears in (29) has a non-linear behaviour which cannot be understood solely by the leaky integrate-and-fire. This is what motivates the introduction of the **Quadratic Integrate-and-Fire**:

$$\frac{dV_M}{dt} = a(I(t) - I_1) + b(V_M - V_1)^2 \tag{34}$$

where a has units of (F^{-1}) and b $(V^{-1} \cdot s^{-1})$ and with I_1, V_1 are all positive parameters.

In the case in which $I(t) = I$, which is the one we will be working from now on, this equation can be analytically solved, but before finding the solution, let us study something about the behaviour of fixed points:

[1] Like Sisyphus, it must repeat the process over and over again without reaching the top of the mountain.

Property 3.3.1. *The equation (34) has two fixed points if $I_1 > I$ and none in the complementary. Their coordinates will be:*

$$V_M^* = V_1 \pm \sqrt{\frac{a}{b}(I_1 - I)}. \tag{35}$$

Proof: Using equation (34), and developing the equation for fixed points we obtain:

$$(V_M - V_1)^2 = \frac{a}{b}(I_1 - I).$$

Because a and b are positive, we know that this equation only has real solutions if $I_1 > I$, and the coordinates of such fixed points will be:

$$V_M = V_1 \pm \sqrt{\frac{a}{b}(I_1 - I)}.$$

□

Property 3.3.2. *If $I_1 > I$, one of the fixed points is stable and attractive and the other is unstable.*

Proof: The derivative of the system with respect to V_M is:

$$J_f(V_M) = 2b(V_M - V_1). \tag{36}$$

Substituting (35) into (36) we obtain:

$$J_f(V_M^*) = \pm 2b\sqrt{\frac{a}{b}(I_1 - I)}.$$

Therefore the one to the left will be attractive and stable and the one to the right unstable. □

Corollary 3.3.1. The system has a **saddle-node** bifurcation in $I = I_1$, $V_M = V_1$.

Property 3.3.3. *When $I_1 < I$ or $I_1 > I$ and $V_M(t_0) > V_1 + \sqrt{\frac{a}{b}(I_1 - I)}$ V is monotonically increasing.*

Lemma 3.3.1. *When $I_1 < I$ or $I_1 > I$ and $V_M(t_0) > V_1 + \sqrt{\frac{a}{b}(I_1 - I)}$ the solution explodes in finite time. Otherwise, it stays finite.*

Proof: The proof of the second affirmation, that is, the case in which $I_1 > I$ and $V(t_0) < V_1 + \sqrt{\frac{a}{b}(I_1 - I)}$, is trivial seeing what we just studied about fixed points.

For the remainder of the proof, $t_0 = 0$.

Equation (34) is a Ricatti differential equation, which we can reduce to:

$$\frac{d^2x}{dt^2} = \gamma^2 x, \qquad \gamma = \sqrt{-ab(I - I_1)}. \tag{37}$$

With the change of variables

$$V_M = V_1 - \frac{1}{xb}\frac{dx}{dt},$$

the solution to equation (37) is:

$$x(t) = Ae^{\gamma t} + Be^{-\gamma t}.$$

Therefore:

$$V_M(t) = V_1 - \frac{\gamma}{b}\left(\frac{\frac{A}{B}e^{\gamma t} - e^{-\gamma t}}{\frac{A}{B}e^{\gamma t} + e^{-\gamma t}}\right).$$

Imposing the initial condition $V_M(0)$ we obtain:

$$\frac{A}{B} = \frac{1 - D}{1 + D}, \qquad D = b\frac{V_M(0) - V_1}{\gamma}.$$

For the solution to explode in finite time, there must be a value of t, let us say T where:

$$\frac{1 - D}{1 + D}e^{\gamma T} + e^{-\gamma T} = 0.$$

Now, we must distinguish between cases.

If $I > I_1$, then γ is pure imaginary and the former equation can be transformed into:

$$\tan(i\gamma T) = \frac{i\gamma}{b(V_M(0) - V_1)}$$

which has a solution because the tangent is surjective.

If $I < I_1$, γ is real and:

$$e^{-2\gamma T} = \frac{D - 1}{1 + D}.$$

As the exponential is positive the equation has a solution if and only if $D \geqslant 1$ which means:

$$D \geqslant 1 \Rightarrow V_M(0) \geqslant V_1 + \sqrt{-\frac{a}{b}(I - I_1)}.$$

Which proves the result.

□

So, what can we do when our model goes to infinity on a common basis? We consider the times at which the solution does this as firing instants and the reset potential is $-\infty$. Then:

Property 3.3.4. *The frequency of firing if $I > I_1$ fulfils the following law:*

$$f \propto \sqrt{I - I_1}.$$

Proof: We know that if $I > I_1$, we can use the equation:

$$tan(i\gamma T) = \frac{i\gamma}{b(V_M(0) - V_1)}$$

to compute the period.

If we impose $V_M(0) = -\infty$ then:

$$tan(i\gamma T) = 0 \Rightarrow T = \frac{\pi}{i\gamma} = \frac{\pi}{\sqrt{ab(I - I_1)}}.$$

Taking the inverse gives us the desired result.

□

Using the parameters:

a	1 F^{-1}
b	1 $mV^{-1} \cdot ms^{-1}$
V_1	0 mV
I_1	2 A

Table 4: Data for the simulations with the Quadratic Integrate-and-fire model.

We can do some simulations to show what we just proved (of course we stop before going to ∞, because we cannot treat that numerically):

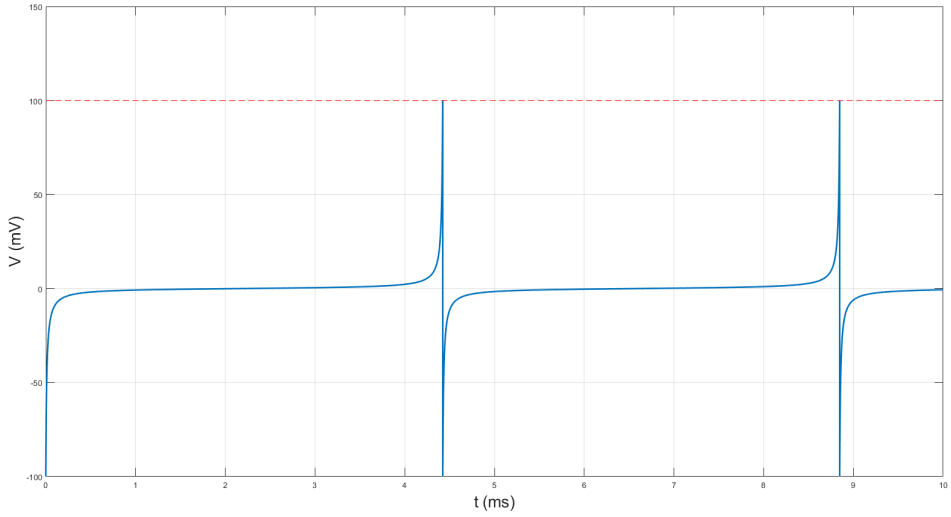

Fig. 27: Simulation of the QIF model with $I = 2.5A$, $V(0) = -\infty$, which is over the threshold. The red dashed line indicates the position of the threshold.

From this we have measured the distance between peaks obtaining an estimate which is near the value that we can calculate using the last property:

$$T_{exp} = 4.42\,\text{ms} \approx 4.44\,\text{ms} = \frac{\pi}{\sqrt{ab(I - I_1)}}$$

which makes sense because of the fact that we stopped the simulation before actually going to infinity, so the simulated period is slightly smaller.

If $I = 1 < I_1$ and the initial condition is between the fixed points we find, as expected:

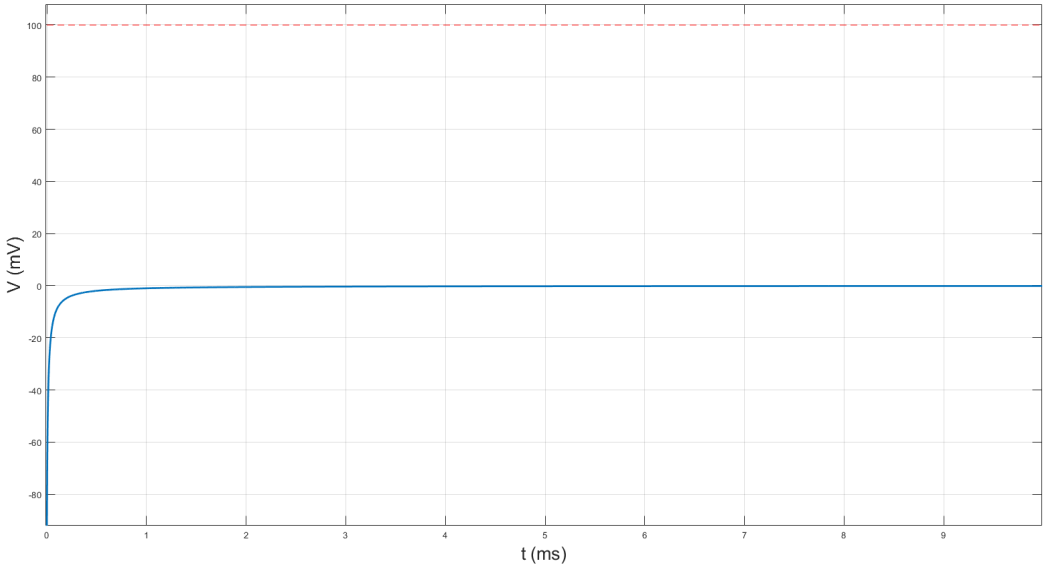

Fig. 28: Simulation of the QIF model with $I = 2A$, $V(0) = -2mV$, which is under the threshold. The red dashed line indicates the position of the threshold.

3.4. θ-model

Let the following change of variables in (34):

$$V_M = V_1 + \frac{c}{b}\tan\left(\frac{\theta}{2}\right)$$

where c is a positive constant (s^{-1}).

Then, it can be found that the equation for $\theta(t)$ is:

$$\frac{d\theta}{dt} = c(1 - cos(\theta)) + \frac{ab}{c}(1 + cos(\theta))(I - I_1). \tag{38}$$

This is the so-called **θ-model**.

This model has very similar characteristics to the ones found in the Quadratic Integrate-and-fire, it has the same properties and the bifurcation point is exactly the same.

Apart from this, we must consider the fact that $\theta(t) \in [-\pi, \pi)$ and the system is said to fire when $\theta = \pi$, restarting it to $-\pi$.

Using the parameters from 4 with $c = 1\, ms^{-1}$.

We can show its behaviour which is very similar to the one we saw before in the Quadratic Integrate-and-fire:

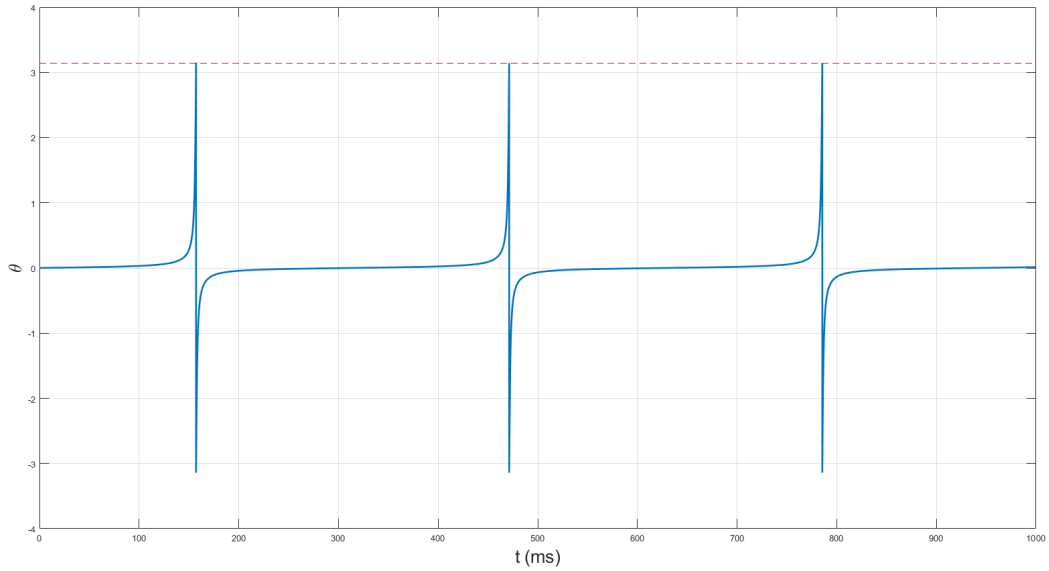

Fig. 29: Simulation of the θ-model under a current $I = 2.5A > I_1$. The red dashed line indicates the position of the threshold.

Part 2. When neurons become noisy: the Fokker-Planck approach.

In this second part, we will now change the scope and will work with a collection of neurons with similar behaviour. In Chapter 4 we will present the mathematical tools needed for this new formalism and deduce a general expression for the Fokker-Planck equation. In Chapter 5 we will explain in depth the arguments that allow us to obtain an equation which can actually be solved and finally, in Chapter 6, we will study the solutions of this equation in different situations.

Many of the proofs and definitions in this chapter have been taken and adapted from [10], [12], [11] and [2].

Chapter 4: Stochastic Calculus

4.1. Random real variables

First, we will present three basic definitions. Our analysis will be unidimensional but can be generalized easily.

Definition 4.1.1 (σ-algebra)**.** Let Ω be a set, then $\mathcal{F} \subset \mathcal{P}(\Omega)$ is a σ-algebra if it has the following properties:

- $\Omega \in \mathcal{F}$.
- $A \in \mathcal{F} \Rightarrow \overline{A} = \Omega \backslash A \in \mathcal{F}$.
- $A,\, B \in \mathcal{F} \Rightarrow A \cup B \in \mathcal{F}$.

Then $(\Omega, \mathcal{F})$ is called a **measurable space**.

One particularly important example of a measurable space is $(\mathbb{R},\, \mathcal{B}(\mathbb{R}))$ where $\mathcal{B}(\mathbb{R})$ is the Borel σ-algebra which is the smallest σ-algebra that contains the euclidean topology in $\mathbb{R}$.

Definition 4.1.2 (Probability function)**.** Let $(\Omega, \mathcal{F})$ be a measurable space, then $P : \mathcal{F} \to [0, 1]$ is a probability function if it has the following properties:

- $\mathrm{P}(\Omega) = 1$.
- Let $\{A_n\}_{n\in\mathbb{N}} \subset \mathcal{F}$ with $A_i \cap A_j = \varnothing$, $i \neq j$ then:

$$P\left(\bigcup_{n=1}^{\infty} A_n\right) = \sum_{n=1}^{\infty} P(A_n)$$

.

We call $(\Omega, \mathcal{F}, P)$ a **probability space**.

Definition 4.1.3 (Real random variable)**.** Let $(\Omega, \mathcal{F})$ and $(\mathbb{R}, \mathcal{B}(\mathbb{R}))$ be measurable spaces and a function $\mathcal{X} : \Omega \to \mathbb{R}$. Then $\mathcal{X}$ is a real random variable if $\mathcal{X}^{-1}(B) = \{\omega \in \Omega : \mathcal{X}(\omega) \in B\} \in \mathcal{F}$, $\forall B \in \mathcal{B}(\mathbb{R})$.

We know that if the space $(\Omega, \mathcal{F})$ has a probability function then $\mathcal{X}$ induces a new probability in $(\mathbb{R}, \mathcal{B}(\mathbb{R}))$:

$$P_{\mathcal{X}}(B) = P(\mathcal{X}^{-1}(B)),\ B \in \mathcal{B}(\mathbb{R}).$$

We will denote the probability of a variable having the value x as $P(x)$.

If our variable is not discrete but continuous, we define the density function:

Definition 4.1.4 (Density Function)**.** If $\mathcal{X}$ is a continuous variable, we call f its density function if:

$$P(\mathcal{X} \in B) = \int_B f(x)dx.$$

Definition 4.1.5 (Expectation value)**.** Let $\mathcal{X}$ be a random variable, then the sum:

$$E(\mathcal{X}) = \sum_j x_j P(\mathcal{X} = x_j) \tag{39}$$

where x_j are the discrete values that the variable can take.

Or, in the case that our variable is continuous:

$$E(\mathcal{X}) = \int_{\mathbb{R}} x f(x)dx \tag{40}$$

where f is the **density function** of $\mathcal{X}$. It is only defined if $E(|\mathcal{X}|)$ is convergent.

We need a last definition to conclude this part:

Definition 4.1.6 (Independent variables)**.** We say that two real random variables $\mathcal{X}$ and $\mathcal{Y}$ are independent if:

$$P(\mathcal{X} \in A,\ \mathcal{Y} \in B) = P(\mathcal{X} \in A)P(\mathcal{Y} \in B),\ \forall A,\ B \in \mathcal{F}.$$

4.2. Basics of stochastic processes

From now on we will be always talking about random variables in a probability space $(\Omega\,, \mathcal{F},\ P)$.

We know that the study of neurons will be time-dependent, as we want to know how the membrane potential will evolve in time, we will study static situations but our main aim is to try and figure out how the distributions will change over time. For this, we need to introduce the concept of a stochastic process:

Definition 4.2.1 (Stochastic process)**.** A stochastic process is a parametrized family of real random variables:

$$\{\mathcal{X}_t\}_{t\in T}$$

where T is the time domain.

So when we think of a stochastic process, we must think about a function of two variables: ω and time. ω can be a lot of things, for instance, a particle. In future chapters, we will work with random variables which represent the membrane potential of a ω neuron at a given time.

Now, we want to figure out the probability of our stochastic variable having a particular value in a particular instant of time. We will call this $P_1(x,t)$.

We can, however, also consider various instants of time $t_1, \cdots, t_n$ in which we want our variable to be $x_1, \cdots, x_n$. We will then call this probability $P_n(x_1\,, t_1;\, x_2\,, t_2;\, \cdots\,;\, x_n,\, t_n)$. We should also consider the fact that there is a hierarchy of these probability functions and that having one we can obtain the ones of lower order just by integrating:

$$P_{n-1}(x_1,\, t_1;\, \cdots\,;\, x_{n-1},\, t_{n-1}) = \int_{\mathbb{R}} P_n(x_1,\, t_1;\, \cdots\,;\, x_n,\, t_n)dx_n. \tag{41}$$

and we can define its expectation value (in the continuous case) as:

Definition 4.2.2 (Expectation value of a stochastic variable)**.** If

$$E(|\mathcal{X}_t|) = \int_{\mathbb{R}} |x|\, P_1(x,t)dx < \infty,$$

then the expectation value of $\mathcal{X}_t$ is defined as:

$$E(\mathcal{X}_t) = \int_{\mathbb{R}} xP_1(x,t)dx.$$

If we have a function $g : \mathbb{R} \times T \to \mathbb{R}$ which is Borel-measurable, then we can define:

$$E(g(\mathcal{X}_t)) = \int_{\mathbb{R}} g(x,t)P_1(x,t)dx$$

if the integral of the absolute value is convergent.

We know that some events can have an effect on future ones. This can be mathematically modelled by the use of conditional probability.

To illustrate this point, let us imagine that our variable has passed through time instants $t_1, \cdots, t_n$ with values $x_1, \cdots, x_n$. Now, this will influence the future probabilities of the process. If we consider l new time steps, we define the **conditional probability** as:

Definition 4.2.3 (Conditional Probability)**.** Let $t_1, \cdots, t_n$ be time instants and $x_1, \cdots, x_n$ values of a stochastic process $\mathcal{X}_t$, if we consider l new time steps and values, we define the

conditional probability of $\mathcal{X}_t$ subjected to $t_1, \cdots, t_n$ and $x_1, \cdots, x_n$ as:

$$P_{l|n}(x_{n+1}, t_{n+1}; \cdots; x_{n+l}, t_{n+l} \,|\, x_1, t_1; \cdots; x_n, t_n) = \frac{P_{n+l}(x_1, t_1; \cdots; x_{n+l}, t_{n+l})}{P_n(x_1, t_1; \cdots; x_n, t_n)}. \tag{42}$$

4.3. Markov processes

We are interested in a specific kind of stochastic process: **Markov processes**. There are many different definitions of such processes but we will use the following:

Definition 4.3.1 (Markov process)**.** We say that a stochastic process $\{\mathcal{X}_t\}_{t\in T}$ is a Markov process if, for each finite time collection $t_1 < \cdots < t_{n-1} < t_n$, the following equation holds:

$$P_{1|n-1}(x_n, t_n \,|\, x_1, t_1, \cdots, x_{n-1}, t_{n-1}) = P_{1|1}(x_n, t_n \,|\, x_{n-1}, t_{n-1}). \tag{43}$$

That is, the probability of the variable's value of being x_n at time t_n only depends on the last known value.

If the probability $P_{1|1}(x_n, t_n \,|\, x_{n-1}, t_{n-1})$ only depends on $\tau = t_n - t_{n-1}$, then we call this Markov process **homogeneous**.

4.3.1. Wiener processes

A very important type of Markov process is the Wiener process, which we are going to use in the future to define stochastic integrals and deduce the Fokker-Planck equation.

They are defined as:

Definition 4.3.2 (Wiener Process)**.** Let W_t be a stochastic process such that:

- $W_0 = 0$.
- Their probability distribution is Gaussian:

$$P_1(x, t) = \frac{1}{\sqrt{2\pi t}} \exp\left(-\frac{x^2}{2t}\right).$$

- For any finite collection of times $t_1 < t_2 < \cdots < t_n$, the random variables $W_{t_j} - W_{t_{j-1}}$ are independent.
- $E(W_t) = 0$ and $E((W_t - W_s)^2) = t - s$, $\forall\, t, s$ such that $0 \leqslant s \leqslant t$.
- $t \to W_t(\omega)$ is continuous for almost all ω.

4.4. Langevin, Itô, Fokker and Planck

Imagine we have a differential equation of the form:

$$\frac{dx}{dt} = A(x,t). \tag{44}$$

In real-life problems, when we are modelling we do not usually have an exact expression of our coefficients as they have some fluctuations or noise:

$$A(x,t) = a(x,t) + noise.$$

Let us call for now $b(x,t)W_t$ the noisy term, where W_t is a stochastic process. We now want to find solutions to the previous equations which are not functions but stochastic processes, due to the introduction of random noise. Let us call the unknown process X_t.

Now, let us consider a discretisation ($0 = t_0 < t_1, \cdots < t_m = t$) in order to approach the solution to the problem:

$$X_{k+1} - X_k = a(X_k,\, t_k)\Delta t_k + b(X_k,\, t_k)\Delta t_k W_k$$

where:

$$X_k = X_{t_k}, \qquad\qquad W_k = W_{t_k}.$$

If we iterate from 0, we arrive at:

$$X_t = X_0 + \sum_{j=0}^{m} a(X_j,\, t_j)\Delta t_j + \sum_{j=0}^{m} b(X_j,\, t_j)\Delta B_j$$

where:

$$\Delta B_j = B_{j+1} - B_j = W_j \Delta t_j.$$

is a Wiener process. The reason behind this is that the characters we observe in many situations conduct us to introduce hypotheses on the noise that are only fulfilled when considering a Wiener process [10].

If we take the limit when $\Delta t_j \to 0$, we know that the first sum turns into a Riemman integral, however, the second sum is somewhat stranger, and it motivates the introduction of stochastic integrals.

The equation (44) after applying the noise is called a **Langevin equation** and noted as:

$$dX_t = a(X_t,\, t)dt + b(X_t,\, t)dW_t. \tag{45}$$

Due to the fact that this work is about neuroscience and not about stochastic calculus, we will introduce the definitions and theorems that we need without proof.

Definition 4.4.1 (Itô integral)**.** Let $f(t)$ a piecewise continuous functions, we define the Itô integral (whenever it converges) as:

$$\int_{t_0}^{t} f(s)dB_s = \lim_{n\to\infty} \sum_{j=0}^{n} f(\tau_j)\Delta B_j$$

where $\tau_j = t_j$.

In the case of (45), we have that:

$$\int_{t_0}^{t} b(X_s,\, s)dB_s = \lim_{n\to\infty} \sum_{j=0}^{n} b(X_{t_j},\, t_j)\Delta B_j.$$

The Itô integral has a very interesting property:

Theorem 4.4.1 (Itô formula)**.** *Let X_t be the solution of an equation as in (45) with bounded coefficients. Let $g(x,t) \in C^2([0,\, \infty) \times \mathbb{R})$ and let us define:*

$$Y_t = g(X_t, t).$$

Then Y_t is the solution of:

$$dY_t = \frac{\partial g}{\partial t}(X_t, t)dt + \frac{\partial g}{\partial x}(X_t, t)dX_t + \frac{1}{2}\frac{\partial^2 g}{\partial x^2}(X_t, t)(dX_t)^2$$

where we must consider:

$$dt \cdot dt = dt \cdot dB_t = dB_t \cdot dt = 0, \qquad dB_t \cdot dB_t = dt.$$

From this, we can finally deduce the **Fokker-Planck equation**.

Theorem 4.4.2 (Fokker-PFlanck equation)**.** *The probability function $P_1(x,t)$ corresponding to the solution of the Langevin equation (45) fulfills:*

$$\frac{\partial P_1(x,t)}{\partial t} = -\frac{\partial (P_1(x,t)a(x,t))}{\partial x} + \frac{1}{2}\frac{\partial^2 (P_1(x,t)b(x,t)^2)}{\partial x^2}$$

for almost all $(x,t) \in \mathbb{R} \times [0,\, \infty)$.

Proof: Let us consider h a function that is only dependent on x and apply Itô's formula:

$$dY_t = \frac{dh(X_t)}{dx}a(X_t,\, t)dt + \frac{dh(X_t)}{dx}b(X_t,\, t)dB_t + \frac{1}{2}\frac{d^2h(X_t)}{dx^2}b^2(X_t,\, t)dt.$$

Taking derivatives with respect to time and taking the expected values from both sides we obtain:

$$\frac{\partial}{\partial t}\int h(x)P_1(x,t)dx = \int \left(\frac{dh}{dx}a(x,t) + \frac{1}{2}\frac{d^2h}{dx^2}b^2(x,t)\right) P_1(x,t)dx.$$

If we do integration by parts on the second side, we obtain:

$$\frac{\partial}{\partial t}\int h(x)P_1(x,t)dx = \int \left[-\frac{d}{dx}(a(x,t)P_1(x,t)) + \frac{1}{2}\frac{d^2}{dx^2}(b^2(x,t)P_1(x,t))\right] h(x)dx.$$

Because the function h is arbitrary, we can just, assuming enough regularity of P_1 move the derivative with respect to time into the integral and obtain the result.

□

We know that the solution of the Fokker-Planck equation is the probability distribution of a Markov process because we have used this hypothesis to deduce it. However, in [10] we can see a Lemma that shows that if the coefficients of the Langevin equation are independent of time, then the process will be time-homogeneous.

Chapter 5: Noisy neurons

We have introduced some mathematical tools that helped us to deduce the Fokker-Planck equation in a general case. However, how does this apply to neural networks? What are we expecting to obtain? Which are the boundary conditions that we must impose for our solution to have physical sense? In this chapter, we will answer all of these questions and give a physical context to mathematics.

5.1. Population activity

There are many, many neurons in the brain (∼100 billion [13]), each of which evolves according to its own dynamics. In reality, our calculations so far have been somewhat anecdotal and illustrative, but if we want to make predictions about the behaviour of the brain in such a way that they can have something to do with the macroscopic sphere and with the data obtained in diagnostic tests, we cannot restrict ourselves to one or two neurons, we have to talk about a significantly larger set of neurons: **Neuronal Populations**.

Each neuronal population comprises neurons that have similar properties and respond in the same way to the same stimuli, which will mathematically translate into their dynamics following the same differential equations. An example of a neuronal population is neighbouring cells in the visual cortex that respond favourably to a given orientation. In this case, the main orientation would be the discrimination criterion that would allow us to define the boundaries of the population.

Let us imagine now that we have a set of N neurons that are part of the same population. Each of them will have its own voltage and will communicate with each other by sending action potentials. If the dynamics of each cell are governed by a system of k equations and we take into account that they are not independent of each other, in order to know the state of the system, that is, the voltages of each of the neurons, we would need to solve a system of k N equations, and knowing that N is usually a huge number, the reader will be able to deduce that this is practically an impossible task.

This situation is very similar to what happened at the dawn of statistical mechanics. When one wants to study the kinetics of gases, one realises that it is impossible to solve Hamilton's equations for systems with such a large number of particles. Thus, we began to work not with microscopic quantities such as the momentum and position of individual molecules, but with macroscopic quantities such as pressure and temperature, deduced from the probability of the particles occupying specific volumes.

We will perform an analogous treatment to this, where the spatial volumes will be replaced by abstract volumes in the dimension of the membrane voltage. Moreover, as we have been introduced in the previous chapter, our treatment will be time-dependent.

But what is the macroscopic quantity we want to measure?

We want a quantity that gives us information about the functioning of a neuronal population, and a way to characterise it. This will be the firing rate of action potentials in the network or **Population Activity**.

There are several ways of defining this firing rate, which we will denote by the letter A.

First, we can think of the most obvious definition:

$$A(t) = \frac{n_{peaks}(t,\, t + T_{test})}{T_{test}} \tag{46}$$

where $n_{peaks}(t, T_{test})$ is the number of peaks between t and t $+T_{test}$.

While this is the most intuitive, it does not really make physical sense, since, in nature, the brain does not wait to estimate the firing rate, because, if it did, phenomena such as reflexes would not exist.

But this is where the role of a large number of neurons in our brain comes into play. Indeed, if we average across our population we get a much simpler and quicker result.

Thus we get a definitive definition of the magnitude to be studied:

Definition 5.1.1 (Population Activity)**.** The activity of a neuronal population with N cells is defined by:

$$A(t) = \lim_{\Delta t \to 0} \frac{n_{peaks}(t,\, t + \Delta t)}{N \Delta t}. \tag{47}$$

And it is measured in Hertz (Hz).

5.2. Mean-Field argument

From now on, we will work with 1D models.

We have already mentioned about the humongous number of neurons that inhabit the brain and even though we are treating a limited portion of them, namely a neuronal population, the number is also large enough to make the treatment of a system of N equations, being N the number of neurons in said population, nearly impossible.

One of the facts that makes this process very difficult is the inability of differentiating between neurons and thus of differentiating between current inputs. This is why we need to resort to stochastic theory and assume that the input current of a neuron is random:

$$I(t) = \mu(t) + \sigma(t) B_t \tag{48}$$

where $\mu(t)$ is the mean, σ the standard deviation and B_t a Wiener process or white noise which we defined before.

For the mathematics of the following sections to be easier and more satisfactory, we will assume that $\mu(t) = \mu$, $\sigma(t) = \sigma$. Even though a time-dependent analysis would prove interesting,

using constant parameters is not a bad approximation based on what is actually observed in experimentation.

Now, if we consider a 1D model whose function does not include the time explicitely:

$$\frac{dV_M}{dt} = F(V_M, I).$$

If we insert equation (48) into the value of I, we obtain a Langevin equation:

$$dV_M = f(V_M, \mu)dt + g(V_M, \sigma)dB_t.$$

And therefore, using the results proven in the former chapter, we obtain the following Fokker-Planck equation for the Langevin equation (5.2):

$$\frac{\partial P(V_M, t)}{\partial t} = -\frac{\partial(f(V_M, \mu)P(V_M, t))}{\partial V_M} + \frac{1}{2}\frac{\partial^2 g(V_M, \sigma)^2 P(V_M, t)}{\partial V_M^2}. \tag{49}$$

This equation will give us the probability of a neuron's membrane voltage of having the value V_M at an instant of time t.

We want to study the ensemble behaviour and for this, we will use arguments inherited from statistical mechanics. We know that the input $I_i(t)$ of a neuron is given by equation (48) and this equation does not contain any reference to the index of the neuron, therefore is independent.

If we assume that the neurons are identical, as they receive the same input, if we study the stationary scenario, we will deduce that the population activity is equal to the firing rate of an individual neuron.

Lemma 5.2.1. *If the activity of a neuronal population $A(t)$ is constant, then it is equal to the firing rate of an individual neuron.*

Proof: Suppose that $A(t) = A_0$.

We know that in a time period T, the N neurons of the neuronal population will produce a number of spikes equal to:

$$n_{spikes}^{network}(T, N) = NTA_0.$$

If we call the stationary value of the firing rate of a neuron f_0, then we know that in the time period T, it will produce:

$$n_{spikes}^{neuron}(T) = Tf_0.$$

Therefore, as all of the neurons are identical, the spatial average that we take in the definition of the population activity (46), we get:

$$A_0 = f_0.$$

□

If we now assume that the dynamics of the system are quasi-stationary, that is, at each time equilibrium is reached, we can assume that the activity of the population, which is a magnitude that averages itself, is equal to the firing rate of a neuron, and the Fokker-Planck equation (49) is used to study it.

The meaning of this new probability density function is the following:

$$\int_{V_1}^{V_2} P(V_M, t) dV_M = \frac{\text{neurons with membrane voltage between } V_1 \text{ and } V_2}{N}.$$

This application of the so-called mean-field arguments is not very rigorous, but it serves to illustrate the main ideas that lead us to disregard the individual character of the neurons that make up the network.

5.3. Boundary conditions, uniqueness and existence

Obviously, we cannot solve this equation as it is, but we need some good boundary conditions.

First of all, it is clear that we have to give it an initial profile $P_0(V_M) = P(V_M, 0)$ to work with, and in the next chapter, we will be testing the effects that are generated depending on the type of temporary initial condition we give.

On the other hand, we know that what we have in hand is a probability distribution. Let Ω be the spatial domain of the solution (which in our case will be unidimensional), we will have to impose that:

$$\int_{\Omega} P(V_M, t) dV_M = 1, \qquad \forall t \in [0, \infty]. \tag{50}$$

If this condition is fulfilled by the initial profile, it suffices to prove that the temporal derivative of the integral is zero.

It is interesting the choice of writing the Fokker-Planck equation (49) as:

$$\frac{\partial P(V_M, t)}{\partial t} = -\frac{\partial J(V_M, t)}{\partial V_M} \tag{51}$$

where

$$J(V_M, t) = f(V_M, \mu) P(V_M, t) - \frac{1}{2} \frac{\partial g(V_M, \sigma)^2 (V_M, t)}{\partial V_M} \tag{52}$$

is a flux of probability.

We have dropped the μ and σ dependency for a neater presentation.

This new form helps us understand the fact that the Fokker-Planck equation is indeed a conservation equation, similar to those of charge or fluid mechanics.

We will be treating two models stochastically: the Leaky Integrate-and-fire (30) and the θ-model (6), which is why we divide the discussion in two parts.

5.3.1. Leaky Integrate-and-fire

Now, we should consider the fact that we will be working with Integrate-and-fire models. In these models, we imposed a threshold for an action potential to be fired. The way to do this was kind of rudimentary: the potential had to be manually reintroduced at the reset voltage V_{reset}. Here, we can impose the threshold by adding a Dirichlet boundary condition:

$$P(V_{th}, t) = 0, \ \forall t \in [0, \infty). \tag{53}$$

From now on, the domain of the solution in the voltage dimension will be $(-\infty, V_{th}]$.

Also, for the probability to be normalisable we need to impose:

$$\lim_{V_M \to -\infty} P(V_M, t) = 0, \ \forall t \in [0, \infty). \tag{54}$$

This condition, in the context of the Fokker-Planck equation, is called an absorbing boundary condition. This is because all points (neurons) that reach the right-hand boundary, the one defined by V_{th}, will vanish. Even if P cancels out at this boundary, there is a non-zero flux J and therefore all neurons passing its refractory period will vanish from our probability distribution, to solve this a delta term is introduced to the equation:

$$\frac{\partial P(V_M, t)}{\partial t} = -\frac{\partial J(V_M, t)}{\partial V_M} + J(V_{th}, t)\delta(V - V_{reset}). \tag{55}$$

Which means that the probability flux leaving on the far right will be reinserted at $V_{reset} < V_{th}$ which is the reset voltage of our neurons.

This term will cause many problems for the numerical solving of the solutions, so we will have to approximate the Dirac delta by a function that resembles it, has integral 1 in the domain of our solution and is smooth enough not to cause us problems. The solution for this is a Gaussian function multiplied by a term that normalises it in our semi-infinite domain. This Gaussian will have a mean V_{reset} and a standard deviation $\sigma_{approx} \sim 0$ which we will adjust according to our needs in future experiments. Thus, the equation (55) is:

$$\frac{\partial P(V_M, t)}{\partial t} = -\frac{\partial J(V_M, t)}{\partial V_M} + J(V_{th}, t)g(V_M) \tag{56}$$

where g is the normalized Gaussian function that we have just defined.

Lemma 5.3.1. *The probability given by equation (56) is conserved when considering the boundary condition (54) at infinity.*

Proof: We can do the following:

$$\frac{\partial}{\partial t}\int_{-\infty}^{V_{th}} P(V_M,t)dV_M = \int_{-\infty}^{V_{th}} \frac{\partial P(V_M,t)}{\partial t}dV_M, \tag{57}$$

due to the fact that the time is not the variable of integration and we assume that P is sufficiently regular. Then, substituting (56) into (57) we obtain:

$$\begin{aligned}\int_{-\infty}^{V_{th}} \frac{\partial P(V_M,t)}{\partial t}dV_M &= -\int_{-\infty}^{V_{th}} \frac{\partial J(V_M,t)}{\partial V_M}dV_M + J(V_{th},t) \\ &= \lim_{V_M\to-\infty} J(V_M,t) + J(V_{th},t) - J(V_{th},t) = \lim_{V_M\to-\infty} J(V_M,t)\end{aligned}$$

where we have used that:

$$\int_{-\infty}^{V_{th}} g(V_M)dV_M = 1.$$

We know that the probability function being 0 at infinity imposes that the J function must also be 0, otherwise, seeing the definition of the flux of probability, the function P would not turn out to be 0. With this, we have the result. □

5.3.2. θ-model

Here things are easier. Let us remember that the θ-model was defined by equation:

$$\frac{d\theta}{dt} = c(1-cos(\theta)) + \frac{ab}{c}(1+cos(\theta))(I-I_1).$$

For now, consider $a = b = c = 1$, $I_1 = 0$.

If we plug (48) into that equation, we obtain the following Langevin equation:

$$d\theta_t = f_1(\theta_t,\mu)dt + f_2(\theta_t,\sigma)dB_t \tag{58}$$

where:

$$f_1(\theta,\mu) = (1-cos(\theta)) + (1+cos(\theta))\mu,\ f_2(\theta,\sigma) = (1+cos(\theta))\sigma,$$

which are both periodic functions. Therefore, the Fokker-Planck equation for the θ model will

have periodic coefficients and it is justifiable to add periodic boundary conditions:

$$\lim_{\theta\to\pi^-} P(\theta,t) = \lim_{\theta\to-\pi^+} P(\theta,t), \tag{59}$$

$$\lim_{\theta\to\pi^-} J(\theta,t) = \lim_{\theta\to-\pi^+} J(\theta,t). \tag{60}$$

and, because of the periodicity of the coefficients and their derivatives, we have:

Property 5.3.1. *The second periodic boundary condition is equivalent to:*

$$\lim_{\theta\to\pi^-} \frac{\partial P(\theta,t)}{\partial\theta} = \lim_{\theta\to-\pi^+} \frac{\partial P(\theta,t)}{\partial\theta}.$$

Then, we have the following:

Lemma 5.3.2. *The solution to the Fokker-Planck equation generated by (58) is conserved with the periodic boundary conditions (59) and (60).*

The proof is analogous to the one in Lemma 5.3.1.

5.4. Analysis of the solutions

We analyze mathematically the solutions for the θ model, as the case of the Leaky Integrate-and-fire includes a term $J(V_M,t)$ which is an evaluation of the solution we are trying to calculate and that ruins our efforts at some previous analysis.

First of all, consider strong solutions to the problem:

$$\frac{\partial P(\theta,t)}{\partial t} = -\frac{\partial(f_1(\theta)P(\theta,t))}{\partial\theta} + \frac{1}{2}\frac{\partial^2(f_2(\theta)^2P(\theta,t))}{\partial\theta^2}. \tag{61}$$

Lemma 5.4.1. *The Fokker-Planck equation (61) with periodic boundary conditions (59) and (60) has an unique strong solution in the domain $[-\pi,\pi]$ if the initial condition $P(\theta,0)=P_0(\theta)$ is analytic.*

Proof: Near $t=0$, the application of **Cauchy-Kovalevska** theorem (Theorem 0.6.5) tells us that the solution exists and is unique, because of the analyticity of the coefficients f_1 and f_2, which are combinations of cosines. If then we consider that probability is conserved, the solution does not blow up and therefore we have global unique solutions.

□

Calculating this solution can be very tedious as we would have to use analytic methods which would yield very complex solutions that are difficult to compute, so we would have to resort to the **weak solutions**. For this, we will use the following theorem found in [15]:

Theorem 5.4.1 (Lions). *Let $V \subset H$ be two separable Hilbert spaces such that V is dense in H.*

Let M, α, $T > 0$, $\beta \geqslant 0$, $F \in L^2(0, T; H)$, $u_0 \in H$ and $a : [0, T] \times V \times V \to V$ a family of bilinear applications, then if:

- $|a(t; u, v)| \leqslant M\|u\|_V\|v\|_V$, $\forall u, v \in V$.
- $a(t; u, v) \geqslant \alpha\|v\|_V^2 - \beta\|v\|_H^2$, $\forall v \in V$.
- $t \to a(t; u, v)$ *is measurable* $\forall u, v \in V$.

Then, the variational problem:

$$\begin{cases} \text{Find } u \in L^2(0, T; V) \cap C^0([0, T]; H) \text{ such that} \\ \frac{d}{dt}(u, v)_H + a(t; u, v) = (F(t), v)_H, \ \forall v \in V, \text{ for almost all } t \in (0, T) \\ u(0) = u_0 \end{cases}$$

has a unique solution.

Now, we can discuss the weak solutions.

Lemma 5.4.2. *The Fokker-Planck equation (61) with periodic boundary conditions (59) and (60) has an unique weak solution in the domain $[-\pi, \pi]$ if the initial condition $P(\theta, 0) = P_0(\theta)$ is in $L^2(\Omega)$.*

Proof: Let us start establishing the settings for the variational problem in which we will transform the PDE.

Take $H = L^2(\Omega)$ where Ω is $[-\pi, \pi]$, and V will be the following subset of **Sobolev space** $H^1(\Omega)$:

$$V = \left\{ v \in H^1(\Omega) \,|\, v(-\pi) = v(\pi) \right\}$$

which is Hilbert because it is closed in $H^1(\Omega)$. The norms in those two spaces are:

$$\|v\|_H = \int_{-\pi}^{\pi} |v(\theta)|^2 \, d\theta.$$

$$\|v\|_V = \int_{-\pi}^{\pi} \left(|v(\theta)|^2 + \left| \frac{dv}{d\theta}(\theta) \right|^2 \right) d\theta.$$

Now, to obtain the bilinear form, we must choose a test function $v \in V$, multiply and then integrate, to obtain (we will drop the dependencies for neatness):

$$\int \frac{\partial P}{\partial t} v + \int \frac{\partial (f_1 P)}{\partial \theta} v - \frac{1}{2} \int \frac{\partial^2 (f_2 P)}{\partial \theta^2} v = 0$$

We analyze now, part by part, the candidates for a and F:

$$\int \frac{\partial^2(f_2 P)}{\partial\theta^2} v = v(\pi)\frac{\partial(f_2 P)}{\partial\theta}(\pi) - v(-\pi) - \frac{\partial(f_2 P)}{\partial\theta}(-\pi) - \int \frac{\partial(f_2 P)}{\partial\theta}\frac{\partial v}{\partial\theta}$$

where we can remove the first part due to the periodic boundary conditions that we imposed in v and in P.

We are left, then with the following applications:

$$F(t) = 0 \tag{62}$$

$$a(t;\, P,\, v) = \int \frac{\partial(f_1 P)}{\partial\theta} v + \frac{1}{2}\int \frac{\partial(f_2 P)}{\partial\theta}\frac{\partial v}{\partial\theta}. \tag{63}$$

About (62) there is not much to talk about, as it is evidently of class L^2.

On the contrary, about (63) we should prove its continuity and the second property of Lions' Theorem because it is obviously bilinear (due to the linearity of the differential and integral operators) and measurable.

For the continuity, considering that f_1 and f_2 are bounded and using the expression of the norms that we discussed above and the Cauchy-Schwarz inequality (Hölder (Theorem 0.6.6) with $p = \frac{1}{2}$), it is trivial.

The second condition is a little bit more difficult to prove:

$$a(t;\, v,\, v) = \int \frac{\partial(f_1 P)}{\partial\theta} v + \frac{1}{2}\int \frac{\partial(f_2 P)}{\partial\theta}\frac{\partial v}{\partial\theta}. \tag{64}$$

First, let us analyze each part:

$$\int \frac{\partial(f_1 v)}{\partial\theta} v = \int f_1' v^2 + \int f_1 \frac{\partial v}{\partial\theta} v = \int f_1 v^2 + \frac{1}{2}\int f_1 \frac{\partial v^2}{\partial\theta}.$$

And now, we can transform this using integration by parts on the second integral, obtaining:

$$\int \frac{\partial(f_1 v)}{\partial\theta} v = \frac{1}{2}\int f_1' v^2.$$

In parallel:

$$\frac{1}{2}\int \frac{\partial(f_2 v)}{\partial\theta}\frac{\partial v}{\partial\theta} = \int f_2' f_2 \frac{\partial v^2}{\partial\theta} + \frac{1}{2}\int f_2^2 (\frac{\partial v}{\partial\theta})^2$$

where the first integral can be transformed into:

$$\int f_2' f_2 \frac{\partial v^2}{\partial\theta} = -\int (f_2^{(2)} f_2 + (f_2')^2) v^2.$$

If we sum and substract:

$$\int f_2^2 v^2.$$

From (64), we will have that:

$$a(t;\, v,\, v) \geqslant \left\| f_2^2 \right\|_\infty \|v\|_V + \int (\cdots) v^2.$$

where the $(\cdots)$ are a combination of sines and cosines and therefore they have a lower bound. If this lower bound is negative, as v^2 is positive, we find the β as minus this lower bound. If this lower bound is positive, we could just take $\beta = 0$ and obtain the desired result.

□

5.5. Stationary Solutions

We know that stationary solutions are to partial differential equations what fixed points are to ordinary differential equations, so it will be useful to have an understanding of these before doing simulations.

5.5.1. Leaky Integrate-and-fire

The Fokker-Planck equation for the LIF model is:

$$\frac{\partial P(V_M, t)}{\partial t} = \frac{1}{\tau_M} \frac{\partial (V_M - V_{rest}) P(V_M, t)}{\partial V_M} + \frac{\sigma^2}{2\tau_M^2} \frac{\partial^2 P(V_M, t)}{\partial V_M^2} + J(V_{th}) g(V_M).$$

If we remove the temporal dependence we obtain:

$$0 = \frac{1}{\tau_M} \frac{d(V_M - V_{rest} - \mu) P_s(V_M)}{dV_M} + \frac{\sigma^2}{2\tau_M^2} \frac{d^2 P_s(V_M)}{dV_M^2} + J(V_{th}) g(V_M),$$

which is linear and therefore has a unique global solution. We will solve this numerically because the term $J(V_{th})$ which depends on the solution makes it impossible to find an analytic solution.

Our domain of integration was infinite, but since we cannot solve numerically in such a domain, we will use a value $-A$ with A large enough to observe the phenomena. This will give us the boundary conditions $P(-A) = P(V_{th}) = 0$ which will allow us to calculate the solutions using the finite difference method.

Another curious numerical detail is the way in which I have calculated the stationary activity A_0 and that is that, inspired by [18], I have left $J(V_{th})$ as a free parameter and adjusted its value so that the norm of 1, which can be done in two steps because the steady state distribution function is directly proportional to the stationary activity, something which also appears in [18].

We use the following data, of which we ignore the units:

μ	3
σ	0.5
σ_{approx}	1
τ_M	0.125
A	-85
V_{reset}	-65
V_{rest}	-65
V_{th}	40
T	2

Table 5: Data for the simulations with the LIF model.

We have chosen the σ_{approx} because it is one order of magnitude below that of the longitude of the voltage domain.

We observe the following profile:

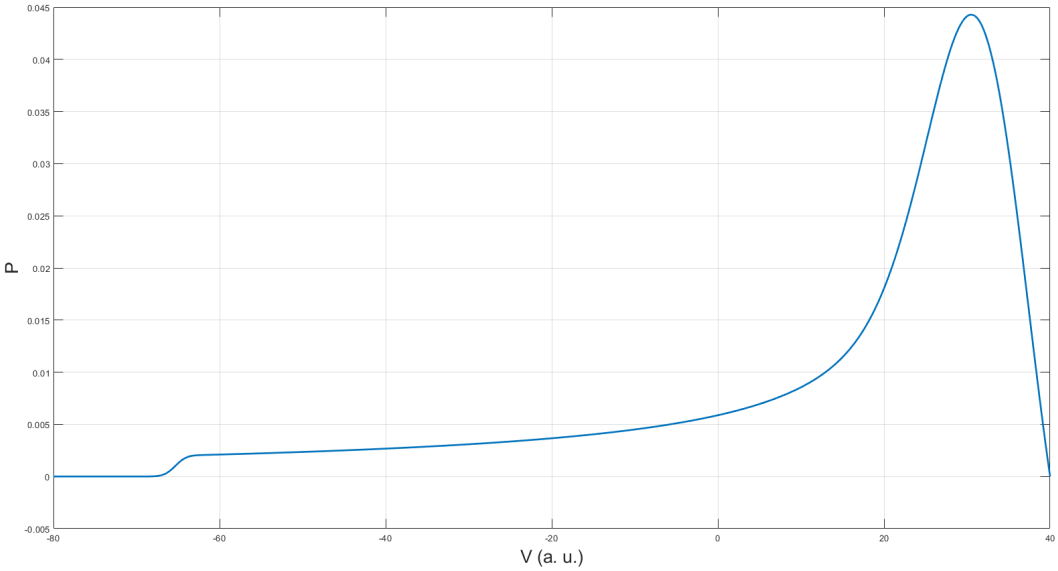

Fig. 30: Steady-state of the LIF model.

For the population activity we simply have to take into account the fact that, by definition, it is the fraction of neurons per unit of time that fire:

$$A(t) = \lim_{V_M \to V_{th}^-} J(V_M, t).$$

With this we obtain a stationary activity:

$$A_0 = 1.59, \tag{65}$$

which should coincide with the limit at large times of the one we calculate.

5.5.2. θ-model

If we erase the time derivative in (61), then we have:

$$0 = \frac{dJ(\theta, t)}{d\theta}.$$

Therefore:

$$J_0 = f_1(\theta)P(\theta) - \frac{1}{2}\frac{dP(\theta)}{d\theta},$$

which gives us an infinitude of solutions.

No more discussion will be done as in a future section we will see that the function does not arrive at any equilibrium.

5.6. Simulations

5.6.1. Leaky Integrate-and-fire

I used a mixed method between explicit Euler and finite differences to calculate the solution. It is important to note how I treated the $J(V_M, t)$ and that is that I did it in two steps. First, I calculated the solution for all voltages and for an instant of time using the J corresponding to the previous instant and then, using those solutions, I obtained a new value for the J with which I calculated the final solution.

Using the data in the table 5 plus the initial condition:

$$P_0(\theta) = \frac{1}{\sigma_{init}\sqrt{2\pi}} \exp(-(x - V_{reset})^2), \qquad \sigma_{init} = 5.$$

We obtain:

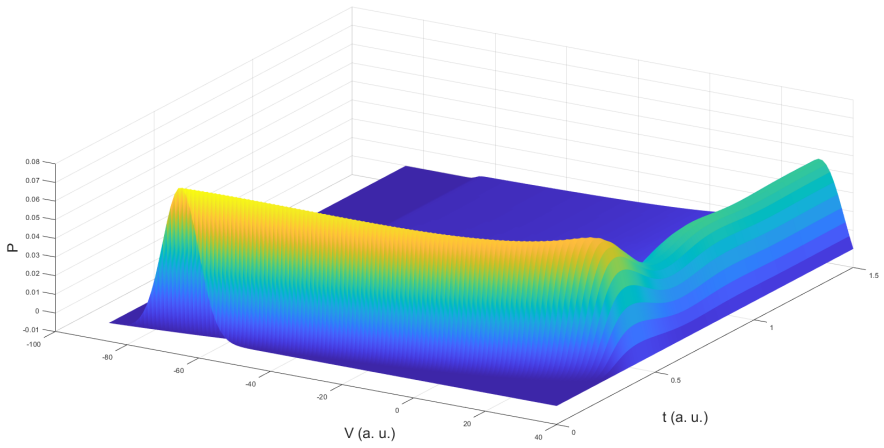

Fig. 31: Probability distribution over time of the LIF neuron model.

where we can see how a steady state is generated when the neurons reach the barrier and then reappear at the reset voltage.

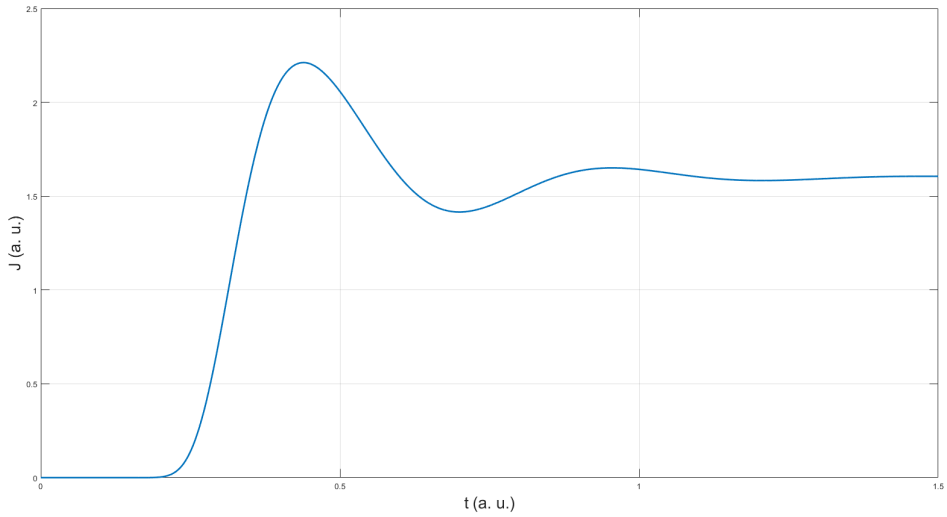

Fig. 32: Population activity over time of the LIF neuron model.

As for their activity, we can see how it approaches a stationary value that practically coincides with the one calculated above (65):

$$A(t \to \infty) = 1.60.$$

If we see how much the solution is worth at the final instant of our simulation, we can observe that it coincides with the calculated stationary solution:

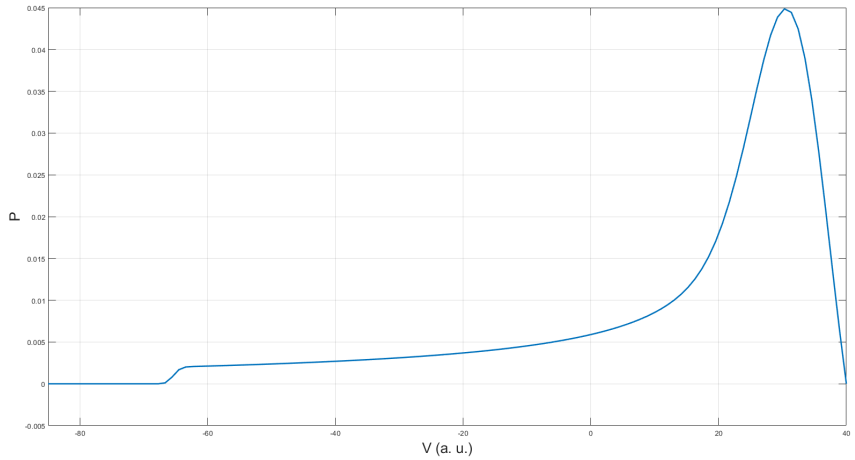

Fig. 33: Probability distribution at time T of the LIF neuron model applied to a neuronal population.

5.6.2. θ-model

We will use the data:

μ	3
σ	0.5
T	2

Table 6: Data for the simulations with the θ model.

and the initial condition:

$$P_0(\theta) = \frac{1}{\sigma_{init}\sqrt{2\pi}} \exp(-\theta^2), \qquad \sigma_{init} = 0.5$$

The selection of these parameters, as in the previous case, is not arbitrary. It is important to choose values that allow for neuron firing while ensuring that the numerical scheme remains stable. This is especially important as the numerical scheme can be very sensitive to small changes, and any divergence could have significant consequences for the accuracy and reliability of the model. Therefore, we carefully considered various factors when selecting these parameters, such as the properties of the neural network and the specific task at hand.

We observe:

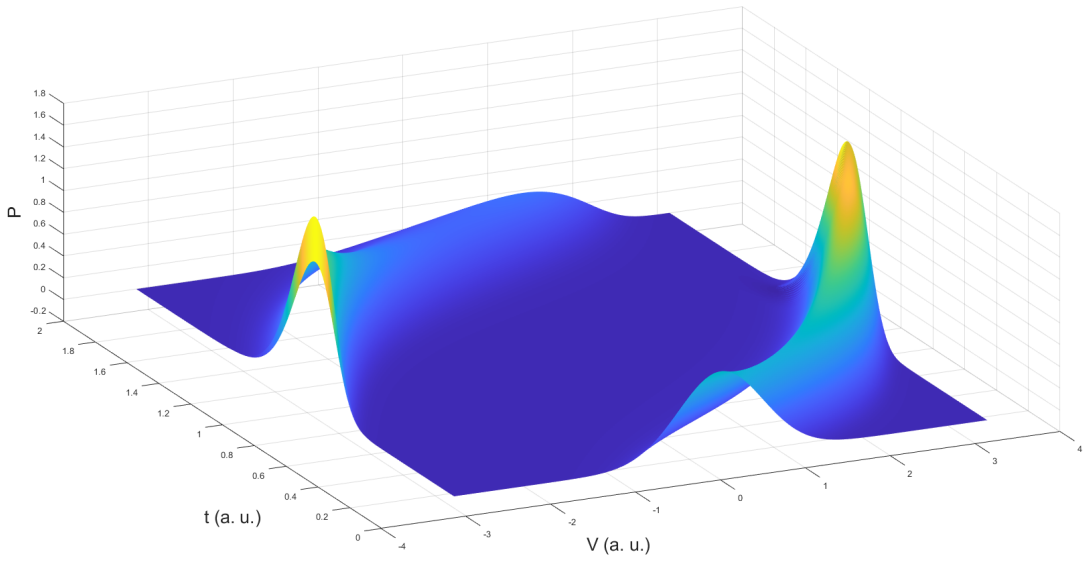

Fig. 34: Probability distribution over time of the θ neuron model applied to a neuronal population.

We have also calculated the values for the activity. Where we only see a peak corresponding to the one in the graph, that is, the moment where almost all of the neurons fire and then go back to the starting point:

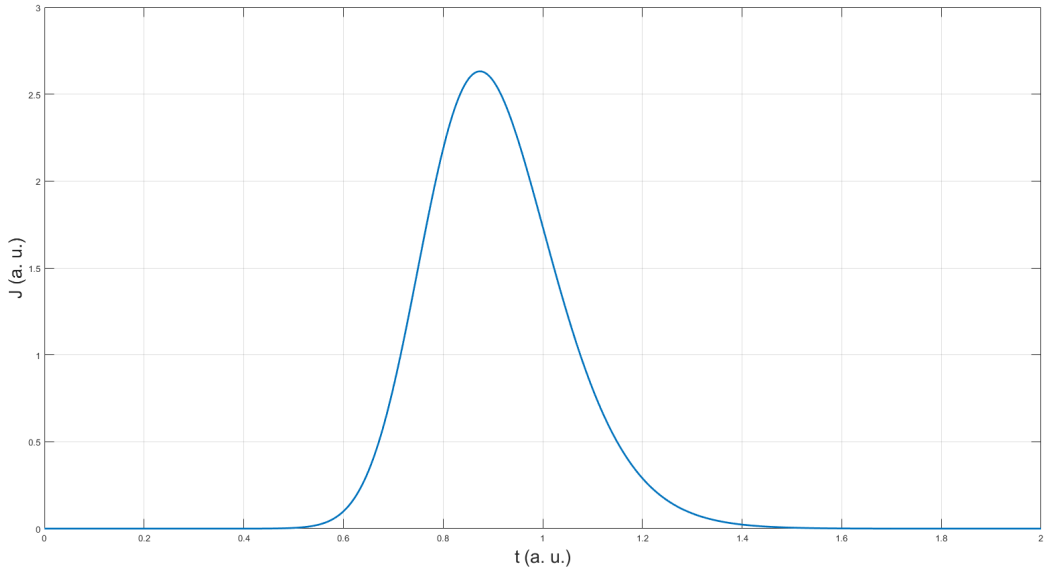

Fig. 35: Population activity over time of the θ neuron model applied to a neuronal population.

We see that the solution is periodic, and the waves will produce indefinitely, however, due to the numerical defects of the scheme we are using, the probability is lost little by little and therefore the wave is fading. The stationary solution is thus never attained in theory. This loss of probability is a function of the number of nodes used in time and in space.

Conclusions

Throughout this work we have seen a staggering variety of neuron models and some so-called neuronal population models for clusters of cells, but there is still a great deal to be seen, many mathematical artefacts of great calibre that, for the brevity of this work, must remain unexamined.

Each chapter of this work acts as a node in the tree of computational neuroscience, because from each small Lemma, equation or concept, a large number of related concepts appear that have been or are being treated by some of the experts in the field, so I wanted to restrict myself to some of the most relevant aspects.

This work does not pretend to be an exhaustive analysis of the subject and to exhaust it, since a field as extensive as this, which is growing day by day, is impossible to cover in so few pages. However, it is a brief introduction to some of the concepts on which current research of such calibre as the European Union's flagship project, **The Human Brain Project**, is based, as well as such fundamental tools in the work of health researchers as **The Virtual Brain**.

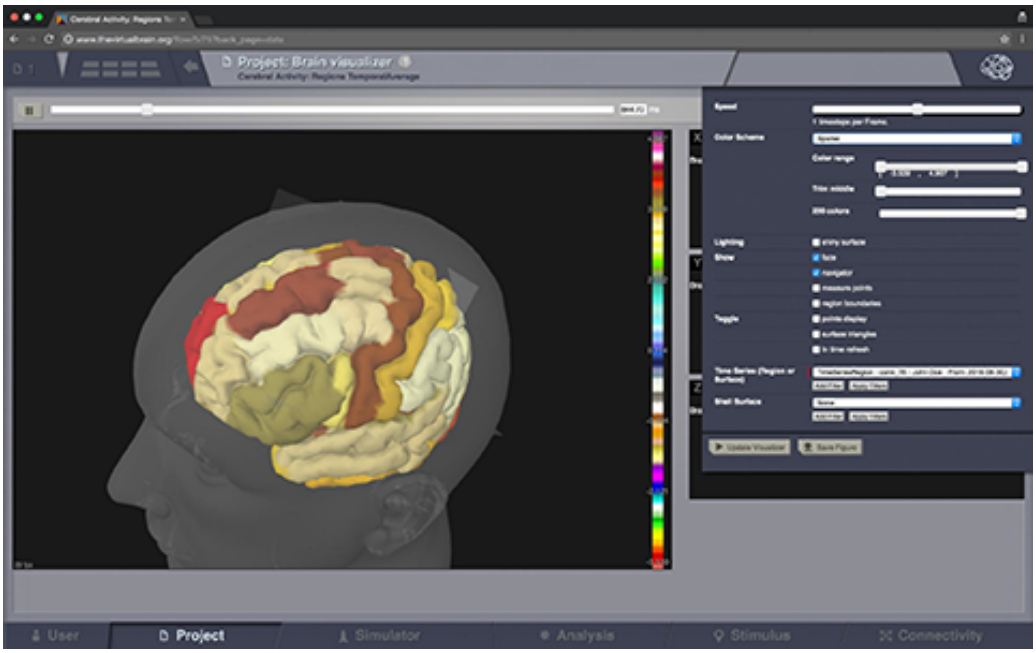

Fig. 36: Simulations of the brain done with The Virtual Brain [19].

We have also neglected concepts such as the detailed study of the waves that travel through the brain, the delayed integrodifferential equations that serve to explain communication over long distances or the models of memories based on neural networks, which are so fashionable today. A good synthesis of most of the knowledge in the field is found in [18] which is a paper that has influenced greatly the structure of this work.

Still, I hope that the reader will be satisfied with my treatment of mathematics and neuroscience and that he or she will have been able to retain some of the ideas that were presented.

Appendix

Simulations code

All of the code for the simulations have been developed by me using MATLAB. As I have used a lot of little scripts and including them here would prolong the work unnecessarily, I link you to my GitHub where I have uploaded everything:

https://github.com/alejbarea/TFGneuroscience.git

Previous mathematical results

We will need some results known to everyone that has taken part in courses on ODEs and stability theory. These will be stated in this section without proof. These results have been extracted from [17] and [16].

Definition 0.6.1 (Hyperbolic fixed point)**.** Let $F : \mathbb{R}^n \to \mathbb{R}^n$ be a dynamical system with a fixed point p. Then if J, the jacobian matrix of F at p, has no eigenvalue with zero real parts then p is hyperbolic.

Theorem 0.6.1 (Local Existence and Uniqueness Theorem)**.** *Let $\Omega \subset \mathbb{R}^{N+1}$ an open set and $f : \Omega \to \mathbb{R}^N$ so that $f \in C^0(\Omega) \cap Lip_{loc}(y; \Omega)$. Under these conditions, for each $(t_0, y_0) \in \Omega$, there exists one and only one maximal solution to the Cauchy Problem:*

$$(CP) \begin{cases} y' = f(t, y) \\ y(t_0) = y_0 \end{cases}$$

Lemma 0.6.1 (Gronwall's Lemma)**.** *Let $0 < t_0 < t_1 < \infty$ and $u, a \in C^0([t_0, t_1])$ with $a(t) \geqslant 0$, $\forall t \in [t_0, t_1]$ and:*

$$u(t) \leqslant M + \int_{t_0}^{t} a(s)u(s)ds, \qquad \forall t \in [t_0, t_1].$$

Then:

$$u(t) \leqslant Me^{\int_{t_0}^{t} a(s)ds}, \qquad \forall t \in [t_0, t_1].$$

Theorem 0.6.2 (Sufficient condition for Lipschitzianity)**.** *Let $\Omega \subset \mathbb{R}^{N+1}$ an open set and*

$$f = (f_1, \cdots, f_N) : \Omega \to \mathbb{R}^N.$$

a function whose partial derivatives $\frac{\partial f_i}{\partial y_j}$ exists and are continuous $\forall i, j = 1, \cdots, N$ then $f \in Lip_{loc}(y, \Omega)$.

Theorem 0.6.3 (Stability by linearization)**.** *Let*

$$y' = f(y)$$

be a differential system with $f \in C^2(B_p)$, $B_p \subset \mathbb{R}^N$, $N \geqslant 1$ a closed ball. Let $y*$ be a critical point of the system, i.e. $f(y*) = 0$. If the eigenvalues of the Jacobian matrix evaluated in $y = y*$, $(\frac{\partial f_i}{\partial y_j}(y*))_{ij}$ have all negative real parts, then $\phi*$, the solution with an initial condition in y $y_0 = y*$, is an exponentially asymptotically stable equilibrium of the system. If any of the eigenvalues has a positive real part, then the equilibrium is unstable.

Theorem 0.6.4 (Poincaré-Bendixon)**.** *Let $y' = f(y)$ be an autonomous system with $f \in C^1(D)$, $D \subset \mathbb{R}^2$ an open and connected non-empty set. Let $y_0 \in K \subset D$ with D a compact that $\gamma^+(y_0) \subset K$ with $\gamma^+(y_0)$ being the orbit of the system starting from t_0. Then, if the set of limit points $\Lambda^+(y_0)$ does not have critical points of the system we have:*

- *$\Lambda^+(y_0)$ is a non-degenerated cyclic orbit.*
- *Either $\gamma(y_0) = \Lambda^+(y_0)$ or $\gamma^+(y_0)$ approaches $\Lambda^+(y_0)$ in spiral motion. In this case we call $\Gamma^+(y_0)$ a **limit cycle**.*

Theorem 0.6.5 (Cauchy-Kovalevska)**.** *A PDE of the form:*

$$\frac{\partial^M u}{\partial x_1^M} = f(x_i,\, u,\, \frac{\partial^{m_1+\cdots+m_n} u}{\partial x_1^{m_1} \cdots \partial x_n^{m_n}})$$

where $m_1 + \cdots + m_n = M$ and boundary conditions for $x_1 = x_1^0$:

$$\frac{\partial^j u}{\partial x_1^j} = L_j(x_2,\, \cdots,\, x_n),\, j = 0,\, \cdots,\, M-1.$$

If f and L_j are analytic in a neighbourhood of $u(x_1^0,\, \cdots,\, x_n^0)$ and $\frac{\partial^{m_1+\cdots+m_n} u}{\partial x_1^{m_1} \cdots \partial x_n^{m_n}}(x_1^0,\, \cdots,\, x_n^0)$ then the equation has an unique local solution in a neighbourhood of $(x_1^0,\, \cdots,\, x_n^0)$.

Theorem 0.6.6 (Hölder)**.** *Let $p,\, q \in (1,\, \infty)$ such that:*

$$\frac{1}{p} + \frac{1}{q} = 1.$$

And $f,\, g : X \to \infty$ are two measurable positive functions over X. Then:

$$\int f g d\mu \leqslant (\int f^p d\mu)^{1/p} (\int f^q d\mu)^{1/q}$$

References

[1] Levitan, I. B., & Kaczmarek, L. K. (2002). The Neuron: Cell and Molecular Biology. Oxford University Press.

[2] Ermentrout, G. B., & Terman, D. H. (2010). Mathematical Foundations of Neuroscience. Springer Publishing.

[3] Strogatz, S. H. (1998). Nonlinear Dynamics and Chaos. En International Workshop. https://doi.org/10.1142/3481.

[4] Hodgkin, A. L., & Huxley, A. F. (1952). A quantitative description of membrane current and its application to conduction and excitation in nerve. The Journal of Physiology, 117(4), 500-544. https://doi.org/10.1113/jphysiol.1952.sp004764.

[5] Izhikevich, E. M. (2006). Dynamical Systems in Neuroscience: The Geometry of Excitability And Bursting (1.a ed.). Mit Pr.

[6] Hartman, P. (1960). A Lemma in the theory of structural stability of differential equations. Proceedings of the American Mathematical Society, 11(4), 610-620. https://doi.org/10.1090/s0002-9939-1960-0121542-7.

[7] Troy, W. C. (1978). The bifurcation of periodic solutions in the Hodgkin-Huxley equations. Quarterly of Applied Mathematics, 36(1), 73-83. https://doi.org/10.1090/qam/472116.

[8] Gerstner, W., Kistler, W. M., Naud, R., & Paninski, L. (2014). Neuronal Dynamics: From Single Neurons to Networks and Models of Cognition. Cambridge University Press.

[9] Novère, N. L. (2012). Computational Systems Neurobiology. Springer Publishing.

[10] Øksendal, B. (2006). Stochastic Differential Equations: An Introduction with Applications. Springer Publishing.

[11] Prados, A. (2022). Ampliación de Física Estadística. Universidad de Sevilla.

[12] Rolls, T., & Deco, G. (2010). The Noisy Brain: Stochastic Dynamics as a Principle of Brain Function. OUP Oxford.

[13] Herculano-Houzel, S. (2009). The human brain in numbers: a linearly scaled-up primate brain. Frontiers in Human Neuroscience, 3. https://doi.org/10.1113/jphysiol.1952.sp004764.

[14] Gardiner, C. W., Gardiner, C. W., & G. (1985). Handbook of Stochastic Methods: For Physics, Chemistry and the Natural Sciences (2nd ed.). Springer.

[15] Fernández Cara, E. (2023). Complementos de Modelización y Optimización numérica. Universidad de Sevilla.

[16] Fernández Cara, E. (2023). Ecuaciones Diferenciales Ordinarias. Universidad de Sevilla.

[17] Romero Enrique, J. M. (2021). Física Matemática. Universidad de Sevilla.

[18] Deco, G., Jirsa, V. K., Robinson, P. N., Breakspear, M., & Friston, K. J. (2008). The Dynamic Brain: From Spiking Neurons to Neural Masses and Cortical Fields. PLOS Computational Biology, 4(8), e1000092. https://doi.org/10.1371/journal.pcbi.1000092

[19] The Virtual Brain. (s. f.). https://www.humanbrainproject.eu/en/medicine/the-virtual-brain/